FKBP52 regulates TRPC3-dependent Ca^{2+} signals and the hypertrophic growth of cardiomyocyte cultures

Sandra Bandleon[1], Patrick P. Strunz[1], Simone Pickel[2], Oleksandra Tiapko[3], Antonella Cellini[1], Erick Miranda-Laferte[2], Petra Eder-Negrin[1*]

[1]From the Comprehensive Heart Failure Center Wuerzburg & the Department of Internal Medicine I, University Hospital Wuerzburg, Am Schwarzenberg 15, 97078 Wuerzburg, Germany; [2]Institute of Physiology, University of Wuerzburg, Röntgenring 9, 97070 Wuerzburg, Germany; [3]Gottfried Schatz Research Center for Cell Signaling, Metabolism and Aging, Medical University of Graz, Austria

[*]To whom correspondence should be addressed: Petra Eder-Negrin, Comprehensive Heart Failure Center Wuerzburg, University Hospital Wuerzburg, Am Schwarzenberg 15, 97078 Wuerzburg, Germany.
eder_p@ukw.de; Tel. (0049) 931-20146510; Fax. (0049) 931-201-646510

Keywords: TRPC3, FKBP, calcineurin, calcium, cardiomyocyte

JCS Advance Online Article. Posted on 20 September 2019

ABSTRACT

The Transient receptor potential (TRP; C-classical; TRPC) channel TRPC3 permeates a cation (Na^+/Ca^{2+}) influx that is favoured by the stimulation of G_q protein-coupled receptors (GPCRs). An enhanced TRPC3 activity is related to adverse effects including pathological hypertrophy in chronic cardiac disease states. In the present study we identified FK506 binding protein 52 (FKBP52) as a novel interaction partner of TRPC3 in the heart. FKBP52 was recovered from a cardiac cDNA library by a C-terminal TRPC3 fragment (amino acids 742-848) in a yeast two-hybrid screen. Downregulation of FKBP52 promoted a TRPC3-dependent hypertrophic response in neonatal rat cardiomyocytes (NRC). A similar effect was achieved by overexpressing PPIase-deficient FKBP52 mutants. Mechanistically, FKBP52 truncated mutants elevated TRPC3-mediated currents and Ca^{2+} fluxes, the activation of calcineurin and the nuclear factor of activated T-cells in NRCs. Our data demonstrate that FKBP52 associates with TRPC3 *via* an as yet undescribed binding site in the C-terminus of TRPC3 and modulates TRPC3-dependent Ca^{2+} signals in a PPIase-dependent manner. This functional interaction might be crucial for limiting TRPC3-dependent signaling during chronic hypertrophic stimulation.

Abbreviations

The abbreviations used are: aa, amino acids; Ang II, angiotensin II; ANP, atrial natriuretic peptide; Co-IP, Co-immunoprecipitation; Ca^{2+} /calmodulin-dependent protein kinase II, CamKII, DAG, diacylglycerol; FK1, FKBP12-like domain 1; FK2, PPIase-like domain 2; FKBP, FK506 binding protein; GAPDH, glycerinaldehyd-3-phosphat-dehydrogenase; GPCR, G_q protein-coupled receptors; HA, hemagglutinin; HDAC4, histone deacetylase 4; HEK 293, human embryonic kidney cells; Hsp90, heat shock protein 90; IP_3, inositol trisphosphate; LP, leucyl-prolyl; mRNA, messenger RNA; NFAT, nuclear factor of activated T-cells; NRC, neonatal rat cardiomyocytes; OAG, Oleoyl-2-acetyl-*sn*-glycerol; PE, phenylephrine; PKC, protein kinase C; PP, peptidyl-prolyl; PPIase, peptidyl-prolyl *cis/trans* isomerase; Pyr3, pyrazole 3; RCAN, regulator of calcineurin 1; Ryr, ryanodine receptor; ßgal, β-galactosidase; TPR, tetratricopeptide; TRPC, transient receptor potential-classical; TRPL, transient receptor potential-like; VP, valyl-prolyl

INTRODUCTION

Transient Receptor Potential (TRP; C-classical; TRPC) channels are tetrameric, non-selective ion channels in the plasma membrane of mammalian cells that are assembled by seven possible subunits (TRPC1-7, TRPC2 is as pseudogene in humans) (Ramsey et al., 2006). As immediate downstream targets of the G_q protein-coupled receptor (GPCR) signaling pathway, they are implicated in a wide range of cellular events in different tissues and organs (Ramsey et al., 2006). Especially in the heart, the stimulation of GPCRs increases a TRPC-mediated Ca^{2+} influx that activates Ca^{2+}-sensitive maladaptive signaling pathways in pathological stress conditions during chronic pressure overload induction or myocardial infarction injury (Eder, 2017; Eder and Molkentin, 2011; Freichel et al., 2017).

A single TRPC subunit is composed of six transmembrane domains with a pore forming loop connecting the transmembrane domains 5 and 6, a preserved 25 amino acid sequence called "TRP" domain and two cytosolic domains, an N-terminal ankyrin repeat domain and a C-terminal coiled-coil domain (Eder et al., 2007; Fan et al., 2018). The cytosolic domains mediate ion channel formation and are implicated in ion channel regulation and plasma membrane targeting (Eder et al., 2007). Among several protein interaction sites, the C-terminus of all TRPC subunits harbours a highly conserved proline-rich sequence that corresponds to the binding domain in the *Drosophila* photoreceptor channel TRPL for the FK506 binding protein 59 (dFKBP59; LPPPFNVLPSVK) (Sinkins et al., 2004; Vazquez et al., 2004), the *Drosophil*a homolog of human FKBP52. The functionally and structurally related subunits TRPC3, 6 and 7 preferably interact with the FKBP isoform FKBP12, and the subunits TRPC1, 4 and 5 with FKBP52 (Sinkins et al., 2004).

Both FKBP12 and FKBP52 are cytosolic proteins that bind the immunosuppressive drug FK506 and function as *cis/trans* isomerases (Bonner and Boulianne, 2017). The isomerase activity is mediated by a peptidyl-prolyl *cis/trans* isomerase (PPIase) site that binds and stabilizes peptidyl-prolyl (PP) bonds in sterically and electrically favourable positions (Lehnart et al., 2003). Also, the activity of TRPC channels is regulated in an isomerase-dependent fashion (Shim et al., 2009). Due to the close resemblance with X-prolyl dipeptides, FK506 disrupts the association between FKBP proteins and their target proteins (Ivery, 2000). Independently of this ability, FK506 exerts immunosuppressive effects by building complexes with FKBP12 which results in the inhibition of calcineurin (Martínez-Martínez and Redondo, 2004). This function is confined to small FKBP proteins but not to the high molecular weight FKBP52 (Erlejman et al., 2014). FKBP52 is mainly known as co-chaperone in heat shock protein 90 (Hsp90)-steroid receptor complexes (Erlejman et al., 2014) and shows a more complex architecture: It contains a catalytic FKBP12-like domain 1 (FK1) including a PPIase site and an FK506 binding pocket, a second PPIase like domain 2 (FK2) without catalytic activity, a domain of three tetratricopeptide (TPR) repeats and a C-terminal calmodulin (CaM)

binding site (Erlejman et al., 2014). The regulation of steroid receptors is dependent on this structural organization. TPR regions in FKBP52 mediate the association with Hsp90 while the FK1 domain in FKBP52 increases receptor transactivation (Sivils et al., 2011) through its isomerase activity.

In the present study we searched for novel modulators and interaction partners of TRPC channels in the heart. We focused on TRPC3 as one of the most relevant isoforms in the maladaptive hypertrophic program during chronic disease states (Kiyonaka et al., 2009; Nakayama et al., 2006; Wu et al., 2010; Zhang et al., 2018). We identified FKBP52 as direct interaction partner of TRPC3, which supports the hypothesis of more promiscuous interactions between TRPC channels and FKBP proteins. As another novel aspect, we found that an association with FKBP52 is mediated by a C-terminal region of TRPC3 outside the putative immunophilin binding region in TRPC3. Our functional analyses further demonstrated that the overexpression of FKBP52 truncated mutants lacking the functional PPIase domain enhanced TRPC3 currents and Ca^{2+} fluxes. In cardiomyocytes, this increase in TRPC3 activity was coupled to an enhanced hypertrophic signaling.

RESULTS

TRPC3 associates through a distal C-terminal region with FKBP52

To identify novel interaction partners of TRPC3 in the heart, we performed a yeast two-hybrid screen known as Ras recruitment system, which is based on the restoration of the Ras signaling transduction pathway in yeast (Aronheim, 2004; Kehat et al., 2011). As baits we used cytosolic regions of human TRPC3 (Accession no. Q13507): an N-terminal protein fragment including the amino acids (aa) 1-341 and two C-terminal fragments covering the proximal (aa 670-797) and the distal C-terminal region (aa 742-848; marked as red bars in Fig. 1A) of TRPC3. The mouse cardiac cDNA library was composed of cDNAs fused to a myristoylation factor which allowed anchorage of the proteins to the cell membrane and interaction with the respective baits in the cytoplasm. With both the N-terminus aa 1-341 and the C-terminal region aa 742-848, positive clones from the cDNA library were recovered (Table 1). The C-terminal region aa 670-797 did not reveal any protein-protein interactions. There were 20-40 repetitive colonies expressing the myosin light chain-related proteins, myosin light chain regulatory B like and myosin light chain polypeptide 2, as well as the triosephosphate isomerase which we considered as non-specific interactions and thus did not include in subsequent investigations. We also found colonies expressing the sarcomeric proteins desmin and myomesin, however, could not validate their interactions with TRPC3 in Co-immunoprecipitation (Co-IP) studies. The recovery of several mitochondrial proteins in the

screen was a surprising finding which could a set a basis for more detailed analyses to elucidate the mitochondrial aspect of TRPC3-dependent Ca^{2+} signaling. There was an interaction with the pre-B-cell leukemia transcription factor interacting protein, an as yet undescribed transcription factor in the heart. Among these candidates, the immunophilin FKBP52 (Accession no. NM_010219) appeared as physiologically relevant interaction partner of TRPC3 given its established role as co-chaperone and ion channel regulator. Another rationale for continuing to analyze the TRPC3-FKBP52 interaction was the fact that FKBP2 was bound to the C-terminal region aa 742-848 (Fig. 1B), which is beyond the putative FKBP binding motif (proline-rich region PP, Fig. 1A), a region that is common in all TRPC isoforms. FKBP52 is composed of an N-terminal FK1 domain with a PPIase active site and an FK506 binding region, an FK2 domain without isomerase activity followed by three TPR1-3 repeats, and a C-terminal CaM binding site (Fig. 1C). The FKBP52 cDNA clone from the yeast two-hybrid screen covered the sequence aa 135-459 including the FK2 domain (aa 167-253), the regions TPR1 (aa 270-303), TPR2 (aa 319-352), TPR3 (aa 353-386) and the C-terminus (Fig. 1C and Fig. S1). The sequence did not contain the isomerase domain FK1 (aa 50-138), except for three amino acids (aa 135-138). Sequence alignment revealed a single point mutation at G1075A, resulting in an amino acid change of R358Q in the TPR3 region of the FKBP52 clone (Fig. 1C and Fig. S1). In Co-IP studies we further analyzed this interaction between the FKBP52 fragment (aa 135-459) from the yeast two-hybrid screen and TRPC3. Confirming the results from the screen, TRPC3 was detected in the immunocomplex of precipitated hemagglutinin (HA)-tagged FKBP52 ((aa 135-459); Fig. 1D). This interaction was comparable to the binding between endogenously expressed FKBP52 and YFP-TRPC3 in HEK 293 cells and in homogenates from mouse hearts (Fig. 1E, F). These results indicate that FKBP52 directly interacts with TRPC3 *via* a non-classical FKBP region in the C-terminus of TRPC3.

Mapping of FKBP52 protein sequences involved in FKBP52-TRPC3 binding

Next, we analyzed which protein structures in FKBP52 mediate the interaction with TRPC3. We constructed five, N-terminally HA-tagged FKBP52 cDNAs covering the following FKBP52 regions: aa 1-138 (PPIase/FK506 domain); aa 139-253 (FK2 domain); aa 230-303 (FK2 and TPR1); aa 280-352 (TPR1 and TPR2); aa 352-459 (TPR3 with the R358Q mutation (marked as red asterisk)) and the C-terminal region of FKBP52 (Fig. 2A). Then we performed Co-IP studies in HEK 293 cells co-expressing YFP-TRPC3 and each of the HA-tagged FKBP52 protein domains by using an HA-antibody. Our Co-IP data showed an interaction between TRPC3 and the FKBP52 fragments aa 1-138, aa 139-253, aa 230-303 and aa 280-352. The C-terminal region of FKBP52 (aa 352-459) containing the mutated TPR3 site and the CaM binding site did not interact with TRPC3 (Fig. 2B,C). This lack of interaction was still observable after back-mutating the FKBP52 fragment (aa 352-459) with the R358Q mutation

to wild-type FKBP52 (Fig. 2D). Based on these data, several regions of FKBP52 associate with TRPC3 including the domains FK1, FK2, TPR1 and TPR2. TPR3 and the C-terminal domain do not interact with TRPC3.

FKBP52 is linked to TRPC3-dependent hypertrophic effects in neonatal rat cardiomyocytes

TRPC3 has been suggested as an important determinant in cardiomyocyte function and Ca^{2+}-dependent signaling mechanisms in the pathological hypertrophic growth of the heart (Eder, 2017; Eder and Molkentin, 2011). We therefore started experiments to analyze whether the pro-hypertrophic effects of TRPC3 were dependent on FKBP52. In a first step, we assessed the hypertrophic growth of cultures from neonatal rat cardiomyocytes (NRCs) treated with FKBP52 siRNAs (Fig. 3A) and with the TRPC3 inhibitor pyrazole 3 (Pyr3) (Kiyonaka et al., 2009). In an agonist-dependent approach, we stimulated the cells with the GPCR agonist phenylephrine (PE) for 24 h. As shown in Fig. 3B and C, PE stimulation resulted in a ~30% enlargement of cardiomyocytes, which was significantly enhanced when FKBP52 was downregulated. When we treated the cells with the TRPC3 inhibitor Pyr3, we found that the hypertrophic increase in scramble (scr) siRNA-treated cells was not affected. In contrast, cardiomyocytes with downregulated FKBP52 expression levels showed a significantly reduced cell size when treated with Pyr3, which was noticeable both at baseline as well as after PE stimulation. These results indicate that an inhibition of TRPC3 attenuates hypertrophy, provided that FKBP52 expression levels are lowered in cardiomyocytes. TRPC6, the structurally and functionally related isoform of TRPC3 was also affected by a downregulation of FKBP52. Hence, overexpression of TRPC6 in NRCs caused a significant baseline hypertrophy which under PE-stimulatory conditions elevated when FKBP52 was downregulated (Fig. S2). These results indicate that there is a functional association not only between FKBP52 and TRPC3 but also TRPC6 which could take place either through a direct binding between FKBP52 and TRPC6 or indirectly through the heteromerization between TRPC3 and TRPC6, a common feature described in several cell types (Dietrich et al., 2005; Strübing et al., 2003; Wu et al., 2010).

The pro-hypertrophic phenotype of NRCs induced by a downregulation of FKBP52 could also be based on mechanisms other than TRPC channel regulation. Hypertrophy implicates a re-arrangement of the cytoskeletal network which includes the stabilization of microtubules. As FKBP52 might play an integral part of microtubule formation (Chambraud et al., 2007) we examined cytoskeletal fractions of NRCs after 24 h of PE stimulation (Fig. S3). Stabilized microtubules are characterized by an increased detyrosination of α-tubulin which results in the removal of the COOH terminal leaving a glutamine on the COOH terminus (Glu-tubulin) (Fassett et al., 2009). Western blotting of cytoskeletal extracts showed that PE stimulation

indeed resulted in increased Glu-tubulin expression levels, however, with no significant differences between scr- and FKBP52 siRNA-treated NRCs (Fig. S3).

Overexpression of FKBP52 truncated mutants promotes cardiomyocyte hypertrophy and calcineurin/NFAT signaling

Analogous to steroid receptors (Sivils et al., 2011), the regulation of TRPC3 by FKBP52 might be divided among different regions in FKBP52. Thus, TPR domains might be involved in the physical association with TRPC3, and the functional PPIase domain in FKBP52 might modulate TRPC3 activity and related hypertrophic mechanisms. Following this hypothesis, we expressed PPIase-deficient structural FKBP52 fragments in order to examine hypertrophy and signaling mechanisms in NRCs. In a first attempt, we infected NRCs with adenoviruses encoding the FKBP52 fragment FKBP52 (aa 135-459) or β-galactosidase (βgal) as control. We then stimulated the cells with PE or the diacylglycerol analogue 1-oleoyl-2-acetyl-*sn*-glycerol (OAG), which is a well-established direct activator of TRPC3 (Tiapko and Groschner, 2018). In both conditions, the hypertrophic enlargement was significantly elevated by FKBP52 (aa 135-459; Fig. 4A,B). Treating NRCs with Pyr3 reversed the pro-hypertrophic effect of FKBP52 (aa 135-459) during stimulation. Notably, adult cardiomyocytes responded with a comparable phenotype which was characterized by an FKBP52 (aa 135-459)-dependent hypertrophic enlargement induced by the stimulation with PE for 24 h (Fig. 4C,D).

To obtain a broader view of GPRCs signaling cascades that are mechanistically connected with TRPC3 we examined NRCs after angiotensin II (Ang II) stimulation. Also, under these stimulatory conditions, FKBP52 (aa 135-459) promoted the hypertrophic response (Fig. S4A) which was linked to tentatively increased expression levels of the hypertrophic marker atrial natriuretic peptide (ANP; Fig. S4B). Interestingly, treatment of NRCs with the immunosuppressant agent FK506 resulted in opposite effects with slightly decreased ANP levels in NRCs (Fig. S4C).

In a next step we examined potential mechanisms that are involved in FKBP52-TRPC3 cardiomyocyte signaling. First, we analyzed the activation of the NFAT isoform NFATc1 by quantifying its relative localization in the cytosol and nucleus of NRCs. There was an increased nuclear localisation of NFATc1-GFP in cells overexpressing FKBP52 (aa 135-459; Fig. 5A,B) or the shorter structural fragment FKBP52 (aa 280-352; Fig. 5C,D). This increased nuclear localization was noticeable at baseline and was reversed by treating the cells with Pyr3. An acute stimulation with the GPCR agonists Ang II or PE did not further promote the activity of NFATc1 (Fig. S5A), a phenomenon that was previously described in rabbit cardiomyocytes (Rinne et al., 2010). Thus, to analyze whether the structural FKBP52 fragments FKBP52 (aa 135-459) and FKBP52 (aa 280-352) also affected calcineurin signaling under stimulatory conditions, we analyzed mRNA levels of the regulator of calcineurin 1 (RCAN) and protein

expression levels of NFATc3, a repeatedly described downstream target of TRPC channels (He et al., 2017; Kuwahara et al., 2006). Interestingly, RCAN was barely upregulated in control-infected NRCs after 24 h of Ang II stimulation, but significantly increased in FKBP52 (aa 135-459)-infected cardiomyocytes (Fig. S5B). To evaluate the effects of FKBP52 (aa 135-459) on NFATc3 expression levels, we isolated nuclear fractions from NRCs. In contrast to NFATc1, NFATc3 was activated during GPCRs stimulation with PE which was displayed by an increased expression of NFATc3 in the nucleus of βgal-infected NRCs and an even further elevation in cells expressing FKBP52 (aa 135-459; Fig. 5E,F).

Based on these data, FKBP52 (aa 135-459) affects calcineurin/NFAT signaling both at baseline and GPCR stimulation but cardiomyocyte hypertrophy only under stimulatory conditions. We therefore hypothesized whether the baseline NFAT activity was not sufficient to induce hypertrophy and required further transcriptional regulators that become activated during GPCR stimulation. We analyzed the expression of the histone deacetylase 4 (HDAC4), a downstream target of the Ca^{2+} /calmodulin-dependent protein kinase II (CamKII), a Ca^{2+}-sensitive regulator of hypertrophy (Backs et al., 2006). Phosphorylation of HDAC4 by CaMKII results in the nuclear export of HDAC4 and a re-expression of genes driving cardiomyocyte hypertrophy. We found slightly decreased expression levels of HDAC4 in nuclear fractions from cells overexpressing FKBP52 (aa 135-459) after PE stimulation and *vice versa* increased HDAC4 expression levels in the cytosol (Fig.5G,H). This adaption might contribute to the hypertrophic profile of cardiomyocytes with elevated FKBP52 (aa 135-459) expression levels.

FKBP52 affects TRPC3-mediated Ca^{2+} signals and ion channel activity

To test the hypothesis of a functional interaction between FKBP52 and TRPC3 as a source of the observed hypertrophic events in cardiomyocytes, we measured cytosolic Ca^{2+} signals in NCRs and HEK 293 cells by applying OAG as TRPC3 activator. In comparison to βgal-infected cells, we found an increased Ca^{2+} influx in cells overexpressing either FKBP52 (aa 135-459) or FKBP52 (aa 280-352; Fig. 6A). Pre-treating the cells with Pyr3 significantly reduced OAG-dependent Ca^{2+} signals (Fig. 6B). The functional link between TRPC3 and FKBP52 was also noticeable in HEK 293 cells. Comparable to the situation in NRCs, TRPC3-mediated Ca^{2+} signals were increased in the presence of FKBP52 (aa 280-352; Fig. 6C,D). Also, Fura 2-AM experiments in a TRPC3 cell line with downregulated FKBP52 expression levels showed the same tendency (Fig. S6A,B). In that case, stimulation of TRPC3 with the GPCR agonist carbachol resulted in a TRPC3-mediated Ca^{2+} influx which was further increased when FKBP52 was downregulated.

In order to gain insight into more direct effects on TRPC3 function, we measured the activity of TRPC3 channels in whole-cell patch-clamp analyses. We transfected HEK 293 cells with YFP-TRPC3, YFP-TRPC3+FKBP52 (aa 280-352) or a YFP-plasmid and elicited TRPC3-

mediated currents with OAG (Tiapko and Groschner, 2018). As shown in Fig. 6, the addition of OAG resulted in a profound increase in current densities in HEK 293 cells expressing YFP-TRPC3 and an even further increase when FKBP52 (aa 280-352) was co-expressed. Co-expression of full-length FKBP52 reversed the stimulatory effect of FKBP52 (aa 280-352; Fig. 6E,F).

FKBP52 truncated mutants do not strengthen the association of TRPC3 with calcineurin, Homer1 or FKBP12

Besides a functional crosstalk, we also considered the possibility of FKBP52 physically interfering with an interaction between TRPC3 and calcineurin. We were interested to find out whether the increased calcineurin activity was based on a tighter association between TRPC3 and calcineurin in the presence of FKBP52 (aa 135-459). According to the quantitative analysis of Co-IP protein fractions, however, FKBP52 (aa 135-459) did not strengthen the association between TRPC3 and calcineurin (Fig. 7A,B).

Previous studies on TRPC1 have identified overlapping binding regions in the N-terminus and the C-terminal immunophilin binding region (LPPPFN) of TRPC1 for FKBP52 and the scaffolding protein Homer (Shim et al., 2009). Functionally, Homer maintains TRPC1 in a closed state and FKBP52 supports an agonist-induced TRPC1 activation (Yuan et al., 2003). Considering such functional constellation, we analyzed whether an interaction between TRPC3 and the PPIase-deficient FKBP52 structural fragments FKBP52 (aa 135-452) and FKBP52 (aa 280-352) resulted in an increased Homer binding in form of a negative-feedback mechanism to prevent over-activation of TRPC3. According to Co-IP studies, there was a weak interaction between TRPC3 and Homer1 which was not affected by the expression of either FKBP52 fragment (Fig. 7C). As another functionally relevant immunophilin, FKBP12 was suggested to associate with TRPC3 (Sinkins et al., 2004) *via* the putative immunophilin binding region located upstream of the region identified in the yeast two-hybrid screen in present study. Thus, we analyzed whether an interaction between the PPIase deficient FKBP52 mutants (aa 135-459 and aa 280-352) and TRPC3 resulted in an increased FKBP12 interaction and thus increased TRPC3 activation as observed in electrophysiology and Ca^{2+} analyses (Fig. 6). Interestingly, we could not detect FKBP12 in TRPC3 precipitates regardless of the expression of FKBP52 (aa 135-459) or FKBP52 (aa 280-352; Fig. 7C).

These results suggest that a PPIase deficiency or loss of total FKBP52 elevates the activity of TRPC3 resulting in elevated Ca^{2+} levels, calcineurin activation and cardiomyocyte hypertrophy.

DISCUSSION

First indications of FKBP proteins as regulatory components in TRPC signalplexes were obtained by functional and biochemical studies in the *Drosophila* brain. In particular, the human FKBP52 homolog dFKBP59 was found to alter TRPL ion channel activation through a direct interaction with a proline-rich domain in the C-terminus of TRPL ((701)LPPPENVLP(709)) (Goel et al., 2001). An almost identical FKBP binding motif, a proline-rich region (PP) in the C-terminus, is present in all seven mammalian TRPC subunits (Sinkins et al., 2004). The first leucyl-prolyl (LP) bond is conserved among TRPC and TRPL channels, whilst the second LP bond is changed to a valyl-prolyl (VP) bond in TRPC3, 6 and 7 and to an isoleucyl-prolyl (IP) bond in TRPC1, 4 and 5. Co-IP studies in insect neuronal cells (Sf9) revealed FK506-sensitive interactions between TRPC channels and FKBPs indicating a role of the C-terminal PP domain as potential binding motif. Furthermore, it was shown that TRPC1, 4 and 5 bind to FKBP52, whereas TRPC3, 6 and 7 to the small FKBP12 in native brain lysates (Sinkins et al., 2004). The reason for this phenomenon has never been entirely resolved. It has been suggested that the 2nd peptidyl-prolyl (PP) bond determines the FKBP selectivity in a similar fashion as observed in the regulation of ryanodine receptors (Ryr). Ryr2 contains an IP bond that is targeted by FKBP12.6 and Ryr1 exhibits a VP dipeptide that interacts with FKBP12 (Gaburjakova et al., 2001). However, a swap of peptide bonds in TRPC3 or TRPC5 failed to alter the binding preference for specific FKBP proteins, giving rise to the speculation that additional regions other than the proline-rich domain are implicated in FKBP interactions. Indeed, C-terminal truncations of TRPL showed that an association with FKBP59 was still possible (Goel et al., 2001).

With our data we confirm this assumption by demonstrating that a C-terminal region of TRPC3 (aa 742-848) directly interacts with FKBP52. With this finding we also oppose previous suggestions that claim an association between selective TRPC subunits and certain FKBP families (Sinkins et al., 2004). We isolated FKBP52 with a TRPC3 protein fragment that does not contain any obvious FKBP binding motifs. The TRPC3 region aa 742-848 that we used as bait in the yeast two-hybrid screen exhibits CaM/inositol trisphosphate (IP_3) binding sites and a coiled-coil domain (Trebak et al., 2005) but lacks PP bonds mediating an FKBP-dependent *cis/trans* isomerization. TRPC3 also does not express a TPR binding motif (MEEVD) that was found to be required for an association between TPR regions in FKBP52 and Hsp proteins in steroid receptor complexes (Erlejman et al., 2014). Interestingly, TRPC3 was directly associated with a truncated FKBP52 protein lacking the PPIase site in the FK1 domain (aa 135-459). When we examined potential TRPC3 binding regions in FKBP52 more closely, we found that several FKBP52 regions were bound to TRPC3. This binding pattern is similar to the interaction between FKBP52 and tubulin (Chambraud et al., 2007). In contrast to the tubulin-FKBP52 association, which requires the TPR domains 1-3 as binding regions, the last

TPR3 region and the C-terminus of FKBP52 (aa 352-459) failed to interact with TRPC3. This was an unexpected finding since several important binding structures are located in this region including a conserved charge-Y motif in the CaM binding domain (aa 410-420) or critical residues in TPR3 (K354A) (Cheung-Flynn et al., 2003). This lack of interaction was independent of the mutation (R358Q) in FKBP52 (aa 352-459) suggesting a negligible role of this region in TRPC3 binding and a more prominent role of protein-protein interaction sites within TPR1 and TPR2.

By following up the functional relevance of this unique TRPC3-FKBP52 assembly, we found a limiting effect of FKBP52 on TRPC3-dependent Ca^{2+} signals and downstream hypertrophic signaling pathways in cardiomyocytes. These assumptions were corroborated by cytosolic Ca^{2+} measurements in HEK 293 cells that showed increased TRPC3-mediated Ca^{2+} signals under FKBP52 downregulated conditions. Also, the small structural FKBP52 fragment (aa 280-352) co-expressed with TRPC3 in HEK 293 cells, elevated an OAG-dependent TRPC3 conductance and Ca^{2+} influx, giving rise to the speculation that an interaction between TRPC3 and FKBP52 (aa 280-352) results in the replacement of endogenously expressed FKBP52 and thus in an alleviation of the inhibitory effect of FKBP52. Further Ca^{2+} studies in NRCs showed that a larger FKBP52 fragment (aa 135-459) had comparable effects on cytosolic Ca^{2+} signals. In line with our observations, *Drosophila* dFKBP59 exerted inhibitory effects on the stimulation and activity of TRPL (Goel et al., 2001). Similarly, it was shown that the open probability of skeletal muscle and cardiac ryanodine receptors was reduced by FKBP12 or FKBP12.6, respectively, and the Ca^{2+} sensitivity of the receptors elevated when FKBP12 or FKBP12.6 were displaced (Lehnart et al., 2003). However, in the setting of TRPC channel regulation, FKBP proteins exerted stimulatory effects on ion channel gating. For example, FK506 treatment resulted in a disruption of TRPC6-FKBP12 binding, and decreased the current density and agonist activation of TRPC6 (Lopez et al., 2015; Sinkins et al., 2004). Regarding the regulation of TRPC1, it was shown that single point mutations in the PPIase domain of FKPB52 (FD67DV) and FKBP12 (D37L) failed to produce a considerable isomerization of N- and C-terminal structures in TRPC1 (Shim et al., 2009). Consequently, the spontaneous activity of TRPC1 was increased by the presence of the isomerase-dead FKBP12 mutation, and an agonist-induced TRPC1 activation was blocked when the catalase-impaired FKPB52 isoform was expressed (Shim et al., 2009). Based on our findings of elevated TRPC3 current densities and Ca^{2+} signals that we elicited by expressing the FKBP52 truncated mutant FKBP52 (aa 280-352), we assume that the activity of TRPC3 is also regulated in an isomerase-dependent fashion, although, in contrast to other mammalian TRPC isoforms, towards an inhibitory functional state. Consequently, due to an impaired interaction with FKBP52, TRPC3 might become more sensitive to stimulation and allow greater Ca^{2+} fluxes. As an additional mechanism in such situations, the *cis/trans* isomerization of TRPC3

through FKBP12 might contribute to an increased TRPC3 activation. FKBP12 was identified as a TRPC3 interaction partner in brain lysates binding to the C-terminal PP motif in TRPC3 (Sinkins et al., 2004). A loss of interaction between TRPC3-FKBP52 might strengthen an association between FKBP12 and TRPC3, resulting in an increased channel activity during stimulation. Surprisingly, we could not detect endogenously expressed FKBP12 in TRPC3 immunoprecipitates, suggesting that the observed functional effects of FKBP52 in HEK 293 cells unlikely involve FKBP12. Our biochemical analyses also excluded the scaffold protein Homer as regulator of a TRPC3-FKBP52 complex. Although TRPC3 was associated with Homer1, the strength of interaction remained unchanged in the presence of FKBP52 structural fragments. Based on this experimental level, Homer1 does not seem to be recruited as a negative feedback mechanism that prevents an over-activation of TRPC3. However, future experiments with reduced Homer or FKB12 levels are required to define the interplay with FKBP52 in HEK 293 as well as native cardiomyocytes.

In cardiomyocytes, the physiological relevance of the FKBP52-TRPC3 coupling became apparent as an elevated agonist-dependent hypertrophic response. The rationale to analyze cardiomyocyte hypertrophy was based on the role of TRPC3 as a crucial mediator in the hypertrophic program translating GPCR stimuli to Ca^{2+}-dependent signaling proteins (Eder, 2017; Eder and Molkentin, 2011). The hypertrophic increase on the cellular level was achieved by an α-adrenergic or Ang II-dependent stimulation of NRCs. Interestingly, the presence of Pyr3, a specific TRPC3 inhibitor (Kiyonaka et al., 2009), reduced the cardiomyocyte enlargement under conditions of an FKBP52 knock-down. Based on these data, a GPCR-dependent hypertrophic enlargement involves some degree of TRPC3 activity, which is further promoted when FKBP52 is downregulated. Importantly, Pyr3 also reduced the cell growth at baseline pointing to a constitutive TRPC3 activity, a commonly described feature of this TRPC isoform (Dietrich et al., 2003). Following our hypothesis and in line with our functional data, the expression of structural FKBP52 domains lacking the PPIase site had similar effects causing an increased cell enlargement with slightly up-regulated ANP expression levels after GPCR stimulation, although without inducing a baseline hypertrophic response. This discrepancy compared to an FKBP52 knock-down remains elusive. It could be based on an increased baseline activity of TRPC3, a tighter association with calcineurin or, speculatively, increased binding of FKBP12.6 that elevates the spontaneous TRPC3 activity as previously shown for TRPC1 in neurons (Shim et al., 2009).

Nevertheless, FKBP52 structural mutants were coupled with an enhanced baseline NFATc1 activation that was diminished by the TRPC3 inhibitor Pyr3. In addition, we observed an altered expressional profile of NFATc3 and HDAC4 that is characteristic of an increased hypertrophic enlargement during GPCR stimulation. Indeed, OAG and PE, as well as Ang II, induced a significant hypertrophic response in adult and neonatal cardiomyocytes when

FKBP52 mutants were expressed. We assume that during agonist activation these structural FKBP52 mutants induce a TRPC3-mediated Ca^{2+} influx that evokes several signaling pathways including calcineurin/NFAT and the CamKII that govern a pro-hypertrophic profile. Interestingly, the treatment of cardiomyocytes with FK506 did not imitate the pro-hypertrophic phenotype of an FKBP52 knock-down by competing FKBP52 off from TRPC3. Since FK506 targets multiple intracellular receptors of the FKBP family, its potential role to displace FKBP52 from TRPC3 might be masked by other mechanisms. FK506 is best-known for its inhibition of calcineurin through a complex formation with FKBP12 (Li et al., 2011), which might be the dominating mechanism causing anti-hypertrophic effects in cardiomyocytes. Indeed, *Gao et al.* (Gao et al., 2012) reported that FK506 blocked hypertrophy and calcineurin/NFAT activity in NRCs which, paradoxically, was induced by overexpressing TRPC3. These effects could very well be determined by a relief of stimulatory effects that are based on an FKBP12 *cis/trans* isomerization of TRPC3. In case of such a scenario, the use of FK506 as calcineurin inhibitor (Wilkins and Molkentin, 2004) needs to be even more carefully evaluated. Referring to the functional relationship between FKBP52 and TRPC3, an inhibition of FKBP52 would most certainly cause adverse effects given its role in preventing calcineurin/NFAT activation and hypertrophy. The concept of this novel mechanism is worth investigating in the intact heart by future studies.

MATERIALS AND METHODS

Yeast two-hybrid growth screen

The Ras recruitment screen was performed as described in (Aronheim, 2004; Kehat et al., 2011). In brief, the bait was a hybrid protein consisting of an activated Ras protein lacking its farnesylation CAAX box and the TRPC3 protein fragments (aa 1-341, 670-797 and 742-848 from the TRPC3 isoform 3/Q13507-3 in Uni Prot.). The bait plasmid was co-transfected into Cdc25-2 yeast cells with a myristoylated heart cDNA library (CryoTrap; Agilent Technologies). The expression of the cDNA library was under the control of the Gal1-inducible promoter, while the expression of the bait was controlled by a Met-off inducible promoter. Plates were incubated at the permissive temperature of 24°C for 7 d, were subsequently replicated onto inductive medium and incubated at the restrictive temperature of 36°C. Colonies with efficient growth were selected and grown on appropriate glucose plates for 2 d. Subsequently, galactose and methionine dependency were assayed by replica plated at the restrictive temperature of 36°C. Colonies that exhibited efficient cell growth and full dependency were further analyzed. The plasmid DNA was isolated, and the library plasmid identified by sequencing. Identified library plasmids were reintroduced into Cdc25-2 cells with the specific bait and the interaction was re-examined using the galactose and methionine dependency test at the restrictive temperature of 36°C.

Molecular biology, adenovirus generation and mRNA analysis

FKBP52 cDNA fragments encoding the aa 1-138; 139-253; 230-303; 280-352; 352-459 and 135-459 were amplified by PCR using mouse FKBP52 as template and subcloned into pcDNA3.1 containing an HA-sequence. For the site-directed mutagenesis of the HA-cDNA fragment encoding FKBP52 (aa 352-459), the instructions of the QuikChange II Site-Directed Mutagenesis Kit from Agilent Technologies were followed. The following primer sequences were included in the PCR reaction: FW: 5'GCCTGTTTCGCCGGGGAGAGGCCCA3'; RV: 5'TGGGCCTCTCCCCGGCGAAACAGGC3'. For the generation of adenoviruses, cDNAs encoding the FKBP52 protein fragments aa 280-352 or aa 135-459 were subcloned into pENTR 3C Dual Selection Vector and recombined with the pAd/CMV/V5-DEST™ vector following the Gateway® Technology (ThermoFisher Scientific).

Reverse transcription was performed using the SuperScript III First-Strand Synthesis System (Thermo Fisher Scientific). Analysis of RCAN messenger RNA (mRNA) expression levels was performed using individual Taqman gene expression assays (Applied Biosystems). mRNA expression was quantified, normalized to glycerinaldehyd-3-phosphat-dehydrogenase (GAPDH), and expressed relative to βgal-infected cells.

HEK 293 culture and transfection

HEK 293 cells were obtained from ATCC (CRL-1573). The stable TRPC3 cell line T3.9 was provided in a collaboration with the Medical University of Graz (Poteser et al., 2006). The cell lines were regularly tested to confirm the absence of mycoplasma (Applichem). The cells were cultured in Dulbecco's Modified Eagle's Medium with high glucose (DMEM; Sigma) supplemented with 10% fetal bovine serum (FBS; Sigma), 100 U/ml penicillin, 100 µg/ml streptomycin (PAN Biotech) at 37°C and 5% CO_2. T3.9 were additionally treated with the antibiotics G418 (0.5 mg/ml; Sigma). HEK 293 cells were transiently co-transfected with HA-tagged FKBP52 protein fragments, human TRPC3-pcDNA3 (a gift from Jeffery Molkentin, Cincinnati Children's Hospital Medical Center, USA), YFP- (human)TRPC3 (a gift from Klaus Groschner, Medical University of Graz) (Lichtenegger et al., 2013), full-length (mouse)FKBP52-pCMV SPORT6 (Open Biosystems) and/or EGFP-(human)calcineurin (Olivares-Florez et al., 2018) using the X-tremeGENE HP DNA Transfection Reagent (Roche) (1:1 ratio of reagent to DNA).

Neonatal and adult rat cardiomyocyte cultures, adenoviral infections and siRNA treatment

All animal experiments were approved by the authority of Unterfranken and the standing authority of the University Hospital of Würzburg (permit number: 55-2-2531.01-77/13). NRCs were isolated from 1-3 day old Wistar rats (Charles River Laboratories). After the decapitation, the hearts were quickly removed and rinsed with ice-cold Ca^{2+} and bicarbonate-free Hanks Hepes buffer (mmol/l: NaCl 137, KCl 5.366, $MgSO_4x7H_2O$ 0.811, Dextrose 5.55, KH_2PO_4 0.44, Na_2HPO_4 0.34, Hepes 20.06; pH 7.4). The subsequent steps of isolation were described previously (Kirschmer et al., 2016) with some variations. The isolated cardiomyocytes were cultured in minimal essential medium (MEM) including 5% FBS (MEM/5% FBS). After 24 h, the cells were washed with PBS and cultured for additional 24 h in MEM/5% FBS. The cells were infected with adenoviruses encoding βgal, N-terminally mouse HA-tagged FKBP52 (aa 280-352 or aa 135-459), human NFATc1-GFP or mouse TRPC6 (from Seven Hills Bioreagents Cincinnati, USA). The titer was determined by using the Quick Titer Adenovirus Titer ELISA Kit (CELL BIOLABS) and the plaque assay (Baer and Kehn-Hall, 2014). The adenoviruses were applied in a MOI of 50-100 and applied in OptiMEM for 4 h and kept in MEM/1% FBS for further 24 h. For the evaluation of agonist-induced hypertrophy, cells were serum-starved for 24 h and stimulated with Ang II (100 nM; Sigma), PE (50 µM; Sigma), OAG (100 µM) or vehicle for 24 h. In some experiments, FK506 (2 µM; Sigma) was added to the cells. To analyze the nuclear translocation of NFATc1, cells were pre-treated with Pyr3 (10 µM; Calbiochem) or vehicle for 6 h and stimulated with Ang II (1 µM), PE (50 µM) or vehicle for 15 min.

To downregulate endogenous FKBP52 in NRCs and T3.9 cells, the ON-TARGETplus SMARTpool FKBP4 (FKBP52) siRNA from Dharmacon was used and transfected using Lipofectamine RNAiMAX (Life Technologies) according to the manufacturer's instructions. As control we used the ON-TARGETplus Non-targeting Pool. After 48 h, the cells were stimulated with PE (50 µM), Pyr3 (10 µM) or vehicle for 24 h followed by immunocytochemistry or Western blotting.

Adult rat cardiomyocytes were isolated from 5 months old female Wister rats (Charles River Laboratories). The rats were anesthetized with 5% Isoflurane in O_2 and a mixture of buprenorphine (0.05 mg/kg body weight) and heparin (500 IU/kg body weight). After opening the thorax, the heart was removed and cannulated through the aorta on a Langendorff apparatus to perform a retrograde perfusion with a buffer containing (in mmol/L: NaCl 113.01, KCl 4.69, KH_2PO_4 0.6, Na_2HPO_4 0.6, $MgSO_4x7H_2O$ 1.22, Phenol red 0.032, $NaHCO_3$ 12.02, $KHCO_3$ 10, HEPES buffer solution 10, Glucose 5.5, Taurine 30, BDM 10). After 4 min, the

perfusion buffer was switched to a digestion buffer containing 0.072 mg/ml Liberase TH (Roche). The enzymatic digestion was continued until the heart became swollen and slightly pale (6-10 min). The atria were removed, and the remaining ventricles were put in a dish containing 5 ml of perfusion buffer. After cutting the tissue, 5 ml stopping buffer (perfusion buffer with 10% FSC, 12.5 µM $CaCl_2$) were added for 5 min until the cells settled down. The supernatant was discarded and the cell pellet resuspended in 10 ml stopping buffer 2 (perfusion buffer with 5% FCS, 12.5 µM $CaCl_2$) to start the Ca^{2+} reintroduction ($CaCl_2$ solution: 50 µl 10 mM, 50 µl 10 mM, 100 µl 10 mM, 30 µl 100 mM, 50 µl 100 mM). After the last step, the cells were resuspended in plating medium (Medium199 (Sigma) supplemented with 5% Fetal Bovine Serum (FBS; Sigma), 50 U/ml penicillin, 50 µg/ml streptomycin (PAN Biotech), 870 nM Insulin (Sigma), 65 nM Transferrin (Sigma), 29 nM Na-Selenite (Sigma), 0.1 % BDM (Sigma-Aldrich)). The isolated cells were cultured for 3 h and infected with adenoviruses encoding βgal or N-terminally HA-tagged FKBP52 (aa 135-459). The adenoviruses were applied in a MOI of 50-100 in culture medium (Medium199 (Sigma) supplemented with 50 U/ml penicillin, 50 µg/ml streptomycin (PAN Biotech), 870 nM insulin (Sigma), 65 nM transferrin (Sigma), 29 nM Na-selenite (Sigma), 25 µM (-)-blebbistatin (Sigma)) for 24 h. The cells were then stimulated with PE (50 µM) or vehicle in culture medium for 24 h.

Immunocytochemistry, cell surface measurements and NFAT translocation

NRCs or adult rat cardiomyocytes were cultured on laminin (BD Sciences) coated coverslips. After adenoviral infection or siRNA transfection, serum starvation and stimulation with Ang II or PE, cells were fixed with 4% paraformaldehyde, washed with PBS, permeabilized with 0.5% Triton X-100 and blocked with a solution containing 1% BSA, 0.1% cold water fish skin gelatine and 1% Tween-20, as described previously (Kirschmer et al., 2016). Cells were then labelled using an antibody against α-actinin (1:200; Sigma) and a secondary antibody (AlexaFluor 568, 1:400; Life Technologies) to visualize cardiomyocytes, as well as 4′, 6-diamidine-2′-phenylindole dihydrochloride (DAPI) to visualize the nucleus (300 nM; Life Technologies). Fluorescence microscopy was performed by using a Zeiss Axiovert 135 microscope (Zeiss Plan Neofluar) or a Leica DMi8 microscope (Leica Microsystems). The NRC size was determined at least in duplicate cell culture dishes of at least three different cardiomyocyte isolations. The cell size of at least 50 cells/cell culture dish was analyzed by using Image J or the LASX software (Leica). Quantification of the nuclear translocation of NFATc1 was determined by measuring the mean grey value of NFATc1-GFP in the nucleus and in the cytoplasm and calculating the quotient of the values. At least 50 cells/cell culture dish in duplicate cell culture dishes of at least three different cardiomyocyte isolations were analyzed by using the LAS X software (Leica). The size of adult rat cardiomyocytes was determined by light microscopy.

Isolation of protein fractions from NRCs

NRCs were treated as described in (Fassett et al., 2009). They were washed once with PBS pH 7.4 at room temperature (RT), treated with lysis buffer, (containing 1% triton X-100, 1m M EDTA, 100 mM NaCl, 1x protease inhibitor cocktail (Roche) and phosphatase inhibitor cocktail set II (Merck Millipore) and phosphatase inhibitor cocktail set IV (Merck Millipore), and 10% glycerol, in 10 mM Tris HCl pH 7.4. Following this procedure, cytosolic and membrane proteins were released. Intact cytoskeleton, adhesion proteins and insoluble nuclear material kept attached to the plate and were collected in 2x SDS loading buffer (4% SDS, 20% glycerol, in 125 mM Tris-HCl pH 6.8) and used for Western blotting.

Co-Immunoprecipitation and Western blotting

Protein lysates from HEK 293 cells and adult mouse hearts (wild-type; FVB/N) were prepared in a buffer containing 50 mM Tris-HCl; 150 mM NaCl; 1% Triton X-100; 0.5 mM DTT and a protease inhibitor cocktail (Roche) as described previously (Kirschmer et al., 2016; Wu et al., 2010). After a step of preclearing with appropriate control IgGs, the lysates were treated with the following antibodies: anti-HA, (santa cruz, #sc-7392), anti-gfp (abcam, #ab290), or anti-FKBP52 (santa cruz, #sc-1803). Western blotting of protein extracts from HEK 293 cells, NRCs and mouse hearts was performed with the following antibodies: anti-FKBP52 (santa cruz, #sc-1803), anti-HA (santa cruz, #sc-7392), anti-HA (Cell Signaling Technology, #3724), anti-gfp (abcam, #ab290), anti-TRPC3 (custom-made; (Poteser et al., 2006)), anti-GAPDH (Millipore, #MAB374), anti-Homer1 (abcam, #ab211415), anti-FKBP12 (Thermo Fisher, #PA1-026A), anti-Tubulin-detyrosinated (merck Millipore, #AB3201), anti-α-Tubulin (Cell Signalling Technology, #2144), anti-Lamin A/C (Cell Signalig Technology, #2032) followed by horseradish peroxidase-conjugated antibodies (ECL Peroxidase labelled anti-rabbit antibody, (GE Healthcare, #NA934); ECL anti-mouse IgG Horseradish Peroxidase linked whole antibody, (GE Healthcare, #NA931)). All 1st antibodies were diluted 1:1000 and the 2nd antibodies 1:3000. All immunoblots were developed by using a chemiluminescence detection system (Biorad).

Cytosolic Ca^{2+} measurements

HEK 293 cells, T3.9 cells or NRCs were cultured on coverslips and loaded with Fura 2-AM (2 µM; Thermo Fischer) and probenecid (0.5 mM; Thermo Fisher) in a nominally Ca^{2+} free normal Tyrode (NT) solution (mmol/L: NaCl 140, KCl 4, $MgCl_2$ 1, Hepes 5, glucose 10; pH 7.4) for 40 min at RT. HEK 293 cells and NRCs were stimulated with OAG (100 µM; Sigma), 3.9 cells were stimulated with Carbachol (300 µM; Sigma) in nominally Ca^{2+}-free conditions, and perfused with 2 mM extracellular $CaCl_2$. Cytosolic Ca^{2+} levels were calculated as the

fluorescence ratio of 340 nm and 380 nm (F340/F380). Measurements were performed by using the “Myocyte and Contractility System” from Ionoptix and data were analyzed by using the IonWizard 6.3 software (Ionoptix). Transfected cells from at least 3 different cultures were included in the analysis.

Electrophysiology

Whole-cell voltage-clamp experiments in HEK 293 cells were performed using a L/A-EPC7-Amplifier (List Medical Electronic) and a Digidata-1322A Digitizer (Axon Instruments) as previously described (Lichtenegger et al., 2013). Standard extracellular and intracellular solutions were used as described in (Lichtenegger et al., 2013). Linear voltage-ramps were applied ranging from -130 to +80mV. Current values were taken at -90 mV (inward) and at +70 mV (outward) and normalized by cell capacitance.

Statistical analysis

Means ± SEM are presented for all data analyses. The two-tailed unpaired Student’s t-test was used to analyze significant differences between two groups. Significant differences between more than two groups were assessed by one-way ANOVA with the Holm-Sidak method. Two-way ANOVA followed by the Holm-Sidak method was used to detect significant differences when variables were dependent on two factors. In Figs 3B, 4B and Fig. S2, the two-way ANOVA/Holm-Sidak method was used to compare data within the control and stimulatory group, respectively, and the two-tailed unpaired Student’s t-test between data of the control and treatment groups. In Fig.2, the Analysis of Variance on Ranks followed by the Dunn’s Method was applied to detect significant differences between the groups. All analyses were performed by using SigmaPlot 13. $P \leq 0.05$ was considered significant.

Acknowledgements: We thank Alice Schaaf, Anna-Karina Lamprecht, Michelle Gulentz, Annette Berbner and Katharina Marnet for their excellent technical assistance. We also thank Dr. Michael Kohlhaas for supporting electrophysiological recordings.

Competing interests: The authors declare that they have no conflicts of interest with the contents of this article.

Funding: This work was supported by grants from the Bundesministerium für Bildung und Forschung (BMBF01 EO1004 and 01EO1505) through the Comprehensive Heart Failure Center and the Deutsche Forschungsgemeinschaft (DFG; ED 266/1-1).

References

Aronheim, A. (2004). Ras signaling pathway for analysis of protein-protein interactions in yeast and mammalian cells. *Methods Mol. Biol.* **250**, 251–262.

Backs, J., Song, K., Bezprozvannaya, S., Chang, S. and Olson, E. N. (2006). CaM kinase II selectively signals to histone deacetylase 4 during cardiomyocyte hypertrophy. *J. Clin. Invest.* **116**, 1853–1864.

Baer, A. and Kehn-Hall, K. (2014). Viral concentration determination through plaque assays: using traditional and novel overlay systems. *J Vis Exp* e52065.

Bonner, J. M. and Boulianne, G. L. (2017). Diverse structures, functions and uses of FK506 binding proteins. *Cell. Signal.* **38**, 97–105.

Chambraud, B., Belabes, H., Fontaine-Lenoir, V., Fellous, A. and Baulieu, E. E. (2007). The immunophilin FKBP52 specifically binds to tubulin and prevents microtubule formation. *FASEB J.* **21**, 2787–2797.

Cheung-Flynn, J., Roberts, P. J., Riggs, D. L. and Smith, D. F. (2003). C-terminal sequences outside the tetratricopeptide repeat domain of FKBP51 and FKBP52 cause differential binding to Hsp90. *J. Biol. Chem.* **278**, 17388–17394.

Dietrich, A., Mederos y Schnitzler, M., Emmel, J., Kalwa, H., Hofmann, T. and Gudermann, T. (2003). N-linked protein glycosylation is a major determinant for basal TRPC3 and TRPC6 channel activity. *J. Biol. Chem.* **278**, 47842–47852.

Dietrich, A., Kalwa, H., Rost, B. R. and Gudermann, T. (2005). The diacylgylcerol-sensitive TRPC3/6/7 subfamily of cation channels: functional characterization and physiological relevance. *Pflugers Arch.* **451**, 72–80.

Eder, P. (2017). Cardiac Remodeling and Disease: SOCE and TRPC Signaling in Cardiac Pathology. *Adv. Exp. Med. Biol.* **993**, 505–521.

Eder, P. and Molkentin, J. D. (2011). TRPC channels as effectors of cardiac hypertrophy. *Circ. Res.* **108**, 265–272.

Eder, P., Schindl, R., Romanin, C. and Groschner, K. (2007). Protein–Protein Interactions in TRPC Channel Complexes. In *TRP Ion Channel Function in Sensory Transduction and Cellular Signaling Cascades* (ed. Liedtke, W. B.) and Heller, S.), p. Boca Raton (FL): CRC Press/Taylor & Francis.

Erlejman, A. G., Lagadari, M., Harris, D. C., Cox, M. B. and Galigniana, M. D. (2014). Molecular chaperone activity and biological regulatory actions of the TPR-domain immunophilins FKBP51 and FKBP52. *Curr. Protein Pept. Sci.* **15**, 205–215.

Fan, C., Choi, W., Sun, W., Du, J. and Lu, W. (2018). Structure of the human lipid-gated cation channel TRPC3. *Elife* **7**,.

Fassett, J. T., Xu, X., Hu, X., Zhu, G., French, J., Chen, Y. and Bache, R. J. (2009). Adenosine regulation of microtubule dynamics in cardiac hypertrophy. *Am. J. Physiol. Heart Circ. Physiol.* **297**, H523-532.

Freichel, M., Berlin, M., Schürger, A., Mathar, I., Bacmeister, L., Medert, R., Frede, W., Marx, A., Segin, S. and Londoño, J. E. C. (2017). TRP Channels in the Heart. In *Neurobiology of TRP Channels* (ed. Emir, T. L. R.), p. Boca Raton (FL): CRC Press/Taylor & Francis.

Gaburjakova, M., Gaburjakova, J., Reiken, S., Huang, F., Marx, S. O., Rosemblit, N. and Marks, A. R. (2001). FKBP12 binding modulates ryanodine receptor channel gating. *J. Biol. Chem.* **276**, 16931–16935.

Gao, H., Wang, F., Wang, W., Makarewich, C. A., Zhang, H., Kubo, H., Berretta, R. M., Barr, L. A., Molkentin, J. D. and Houser, S. R. (2012). Ca(2+) influx through L-type Ca(2+) channels and transient receptor potential channels activates pathological hypertrophy signaling. *J. Mol. Cell. Cardiol.* **53**, 657–667.

Goel, M., Garcia, R., Estacion, M. and Schilling, W. P. (2001). Regulation of Drosophila TRPL channels by immunophilin FKBP59. *J. Biol. Chem.* **276**, 38762–38773.

He, X., Li, S., Liu, B., Susperreguy, S., Formoso, K., Yao, J., Kang, J., Shi, A., Birnbaumer, L. and Liao, Y. (2017). Major contribution of the 3/6/7 class of TRPC channels to myocardial ischemia/reperfusion and cellular hypoxia/reoxygenation injuries. *Proc. Natl. Acad. Sci. U.S.A.* **114**, E4582–E4591.

Ivery, M. T. (2000). Immunophilins: switched on protein binding domains? *Med Res Rev* **20**, 452–484.

Kehat, I., Accornero, F., Aronow, B. J. and Molkentin, J. D. (2011). Modulation of chromatin position and gene expression by HDAC4 interaction with nucleoporins. *J. Cell Biol.* **193**, 21–29.

Kirschmer, N., Bandleon, S., von Ehrlich-Treuenstätt, V., Hartmann, S., Schaaf, A., Lamprecht, A.-K., Miranda-Laferte, E., Langsenlehner, T., Ritter, O. and Eder, P. (2016). TRPC4α and TRPC4β Similarly Affect Neonatal Cardiomyocyte Survival during Chronic GPCR Stimulation. *PLoS ONE* **11**, e0168446.

Kiyonaka, S., Kato, K., Nishida, M., Mio, K., Numaga, T., Sawaguchi, Y., Yoshida, T., Wakamori, M., Mori, E., Numata, T., et al. (2009). Selective and direct inhibition of TRPC3 channels underlies biological activities of a pyrazole compound. *Proc. Natl. Acad. Sci. U.S.A.* **106**, 5400–5405.

Kuwahara, K., Wang, Y., McAnally, J., Richardson, J. A., Bassel-Duby, R., Hill, J. A. and Olson, E. N. (2006). TRPC6 fulfills a calcineurin signaling circuit during pathologic cardiac remodeling. *J. Clin. Invest.* **116**, 3114–3126.

Lehnart, S. E., Huang, F., Marx, S. O. and Marks, A. R. (2003). Immunophilins and coupled gating of ryanodine receptors. *Curr Top Med Chem* **3**, 1383–1391.

Li, H., Rao, A. and Hogan, P. G. (2011). Interaction of calcineurin with substrates and targeting proteins. *Trends Cell Biol.* **21**, 91–103.

Lichtenegger, M., Stockner, T., Poteser, M., Schleifer, H., Platzer, D., Romanin, C. and Groschner, K. (2013). A novel homology model of TRPC3 reveals allosteric coupling between gate and selectivity filter. *Cell Calcium* **54**, 175–185.

Lopez, E., Berna-Erro, A., Salido, G. M., Rosado, J. A. and Redondo, P. C. (2015). FKBP25 and FKBP38 regulate non-capacitative calcium entry through TRPC6. *Biochim. Biophys. Acta* **1853**, 2684–2696.

Martínez-Martínez, S. and Redondo, J. M. (2004). Inhibitors of the calcineurin/NFAT pathway. *Curr. Med. Chem.* **11**, 997–1007.

Nakayama, H., Wilkin, B. J., Bodi, I. and Molkentin, J. D. (2006). Calcineurin-dependent cardiomyopathy is activated by TRPC in the adult mouse heart. *FASEB J.* **20**, 1660–1670.

Olivares-Florez, S., Czolbe, M., Riediger, F., Seidlmayer, L., Williams, T., Nordbeck, P., Strasen, J., Glocker, C., Jänsch, M., Eder-Negrin, P., et al. (2018). Nuclear calcineurin is a sensor for detecting Ca2+ release from the nuclear envelope via IP3R. *J. Mol. Med.* **96**, 1239–1249.

Poteser, M., Graziani, A., Rosker, C., Eder, P., Derler, I., Kahr, H., Zhu, M. X., Romanin, C. and Groschner, K. (2006). TRPC3 and TRPC4 associate to form a redox-sensitive cation channel. Evidence for expression of native TRPC3-TRPC4 heteromeric channels in endothelial cells. *J. Biol. Chem.* **281**, 13588–13595.

Ramsey, I. S., Delling, M. and Clapham, D. E. (2006). An introduction to TRP channels. *Annu. Rev. Physiol.* **68**, 619–647.

Rinne, A., Kapur, N., Molkentin, J. D., Pogwizd, S. M., Bers, D. M., Banach, K. and Blatter, L. A. (2010). Isoform- and tissue-specific regulation of the Ca(2+)-sensitive transcription factor NFAT in cardiac myocytes and heart failure. *Am. J. Physiol. Heart Circ. Physiol.* **298**, H2001-2009.

Shim, S., Yuan, J. P., Kim, J. Y., Zeng, W., Huang, G., Milshteyn, A., Kern, D., Muallem, S., Ming, G. and Worley, P. F. (2009). Peptidyl-prolyl isomerase FKBP52 controls chemotropic guidance of neuronal growth cones via regulation of TRPC1 channel opening. *Neuron* **64**, 471–483.

Sinkins, W. G., Goel, M., Estacion, M. and Schilling, W. P. (2004). Association of immunophilins with mammalian TRPC channels. *J. Biol. Chem.* **279**, 34521–34529.

Sivils, J. C., Storer, C. L., Galigniana, M. D. and Cox, M. B. (2011). Regulation of steroid hormone receptor function by the 52-kDa FK506-binding protein (FKBP52). *Curr Opin Pharmacol* **11**, 314–319.

Strübing, C., Krapivinsky, G., Krapivinsky, L. and Clapham, D. E. (2003). Formation of novel TRPC channels by complex subunit interactions in embryonic brain. *J. Biol. Chem.* **278**, 39014–39019.

Tiapko, O. and Groschner, K. (2018). TRPC3 as a Target of Novel Therapeutic Interventions. *Cells* **7**,.

Trebak, M., Hempel, N., Wedel, B. J., Smyth, J. T., Bird, G. S. J. and Putney, J. W. (2005). Negative regulation of TRPC3 channels by protein kinase C-mediated phosphorylation of serine 712. *Mol. Pharmacol.* **67**, 558–563.

Vazquez, G., Wedel, B. J., Aziz, O., Trebak, M. and Putney, J. W. (2004). The mammalian TRPC cation channels. *Biochim. Biophys. Acta* **1742**, 21–36.

Wilkins, B. J. and Molkentin, J. D. (2004). Calcium-calcineurin signaling in the regulation of cardiac hypertrophy. *Biochem. Biophys. Res. Commun.* **322**, 1178–1191.

Wu, X., Eder, P., Chang, B. and Molkentin, J. D. (2010). TRPC channels are necessary mediators of pathologic cardiac hypertrophy. *Proc. Natl. Acad. Sci. U.S.A.* **107**, 7000–7005.

Yuan, J. P., Kiselyov, K., Shin, D. M., Chen, J., Shcheynikov, N., Kang, S. H., Dehoff, M. H., Schwarz, M. K., Seeburg, P. H., Muallem, S., et al. (2003). Homer binds TRPC family channels and is required for gating of TRPC1 by IP3 receptors. *Cell* **114**, 777–789.

Zhang, Y., Knight, W., Chen, S., Mohan, A. and Yan, C. (2018). Multiprotein Complex With TRPC (Transient Receptor Potential-Canonical) Channel, PDE1C (Phosphodiesterase 1C), and A2R (Adenosine A2 Receptor) Plays a Critical Role in Regulating Cardiomyocyte cAMP and Survival. *Circulation* **138**, 1988–2002.

Figures

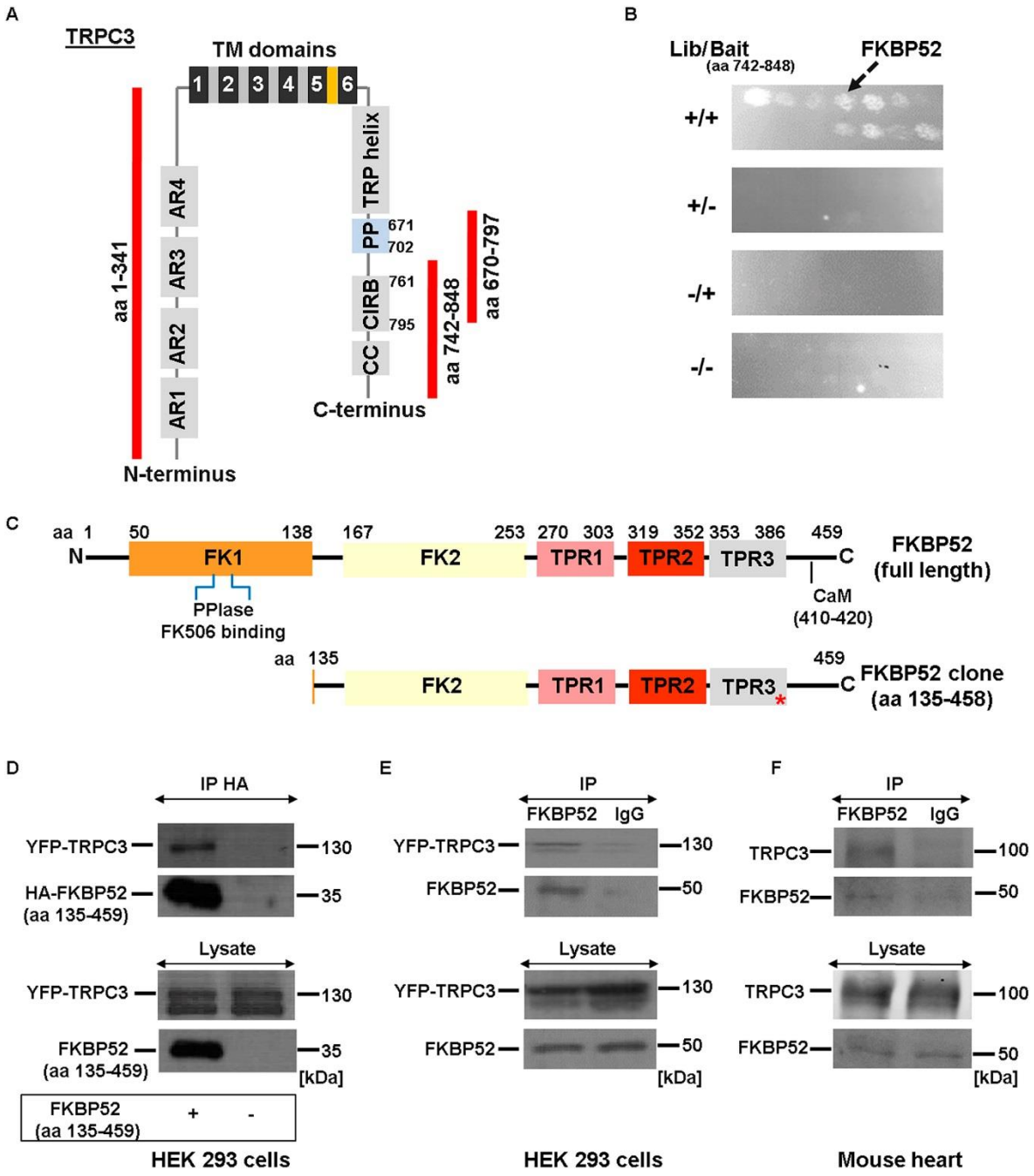

Fig. 1. FKBP52 identified as novel interaction partner of TRPC3 in the heart. (A) Scheme of a single TRPC3 subunit and its structural organization: Shown are the N-terminus with AK1-4 (ankyrin repeats 1-4), 6 TM (transmembrane) domains with the pore region marked in yellow and the C-terminus with a TRP helix, PP (proline rich) region, CIRB (calmodulin/IP_3 receptor binding) and a CC (coiled-coil) domain. The red bars indicate the protein fragments (aa 1-341, 670-797, 742-848) used as baits in the Ras recruitment yeast two-hybrid screen. (B) A yeast

two-hybrid growth assay with the C-terminal TRPC3 protein fragment aa 742-848 revealed the immunophilin FKBP52 as direct interaction partner of TRPC3. Yeast cells were co-transfected with TRPC3 (aa 742-848 (bait)) and a cardiac mouse cDNA library as prey (Lib). Cells were grown on select media to induce the expression of Lib and bait (+/+), Lib (+/-; negative control), bait (-/+; negative control), or neither Lib nor bait (-/-), respectively. Growth of the cells expressing Lib and bait (+/+) reflected a direct protein-protein interaction. (C) Scheme of FKBP52. FK1 (FKBP12-like domain 1; amino acids (aa) 50-138) comprises the peptidyl-prolyl *cis/trans* isomerase (PPIase) and FK506 binding pocket which is followed by FK2 (FKBP12-like domain 2, aa 167-253), three TPR (tetratricopeptide) repeats (TPR1: aa 270-303; TPR2: aa 319-352; TPR3: aa 353-386) and a C-terminus with a calmodulin (CaM) binding site. Note the shortage of the FK1 domain and the point mutation (R358Q; marked as red asterisk) in the FKBP52 protein from the yeast two-hybrid screen. (D) HEK 293 cells were transfected with the HA-tagged FKBP52 fragment (aa 135-459) or vector control (HA-pcDNA3.1) together with YFP-TRPC3 to immunoprecipitate HA-FKBP52 (aa 135-459) and detect YFP-TRPC3 or HA-FKBP52, respectively. (E) Interaction between YFP-TRPC3 and natively expressed FKBP52, as confirmed by IP of FKBP52 or control IgG and consecutive detection of YFP-TRPC3 in HEK 293 cells. (F) Co-IP of FKBP52 and TRPC3 in mouse cardiac lysates. (D-F) Representative Western blots from three independent experiments.

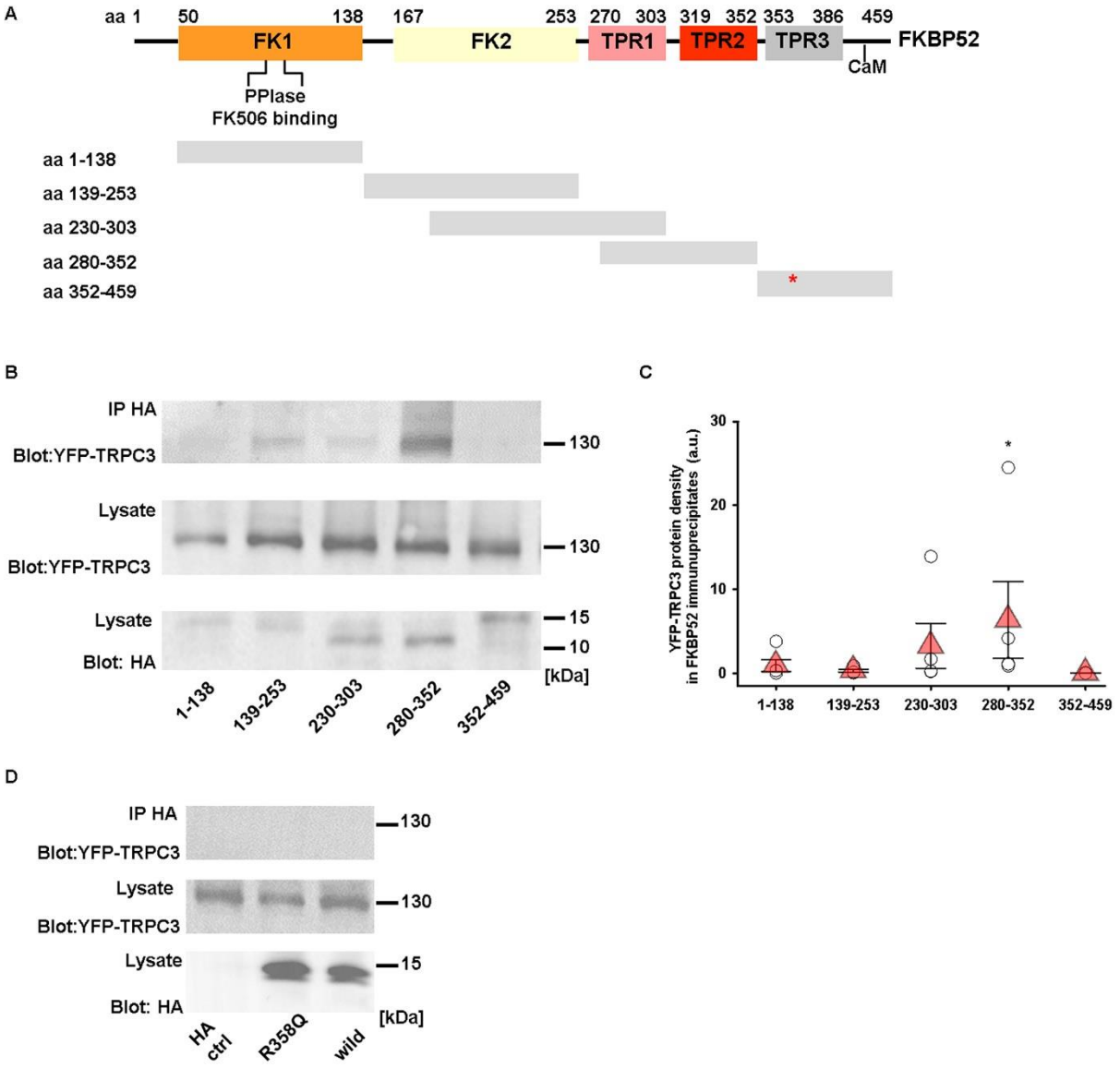

Fig. 2. Identification of FKBP52 sequences involved in FKBP52-TRPC3 binding. (A) Protein structure of FKBP52 with corresponding protein fragments used for Co-IP studies in HEK 293 cells. Schematic of the domains in FKBP52: FK1 (FKBP12-like domain 1 with the peptidyl-prolyl *cis/trans* isomerase (PPIase)) and FK506 binding pocket; FK2 (FKBP12-like domain 2), three TPR (tetratricopeptide) repeats, TPR1-3, and a C-terminus with a calmodulin (CaM) binding site. The red asterisk marks the point mutation R358Q in FKBP52. (B) HA-tagged FKBP52 protein fragments aa 1-138, 139-253, 230-303, 280-352 and 352-459 were expressed together with YFP-TRPC3 in HEK 293 cells. Immunoblots were probed with anti-YFP or anti-HA antibodies, respectively. (C) Protein expression levels of YFP-TRPC3 after Co-IP with different HA-tagged FKBP52 fragments. *P<0.05 vs. 352-459 (Analysis of Variance on Ranks followed by the Dunn's Method), *n* = 5, mean ± SEM. (D) Co-IP of YFP-TRPC3 in

HEK-293 cell lysates expressing YFP-TRPC3 together with HA-FKBP52 (aa 352-459) including the mutation R358Q, wild-type HA-FKBP52 (aa 352-459; wild) or HA-vector control (HA ctrl). An HA-antibody was used for the IP. (B and D) The blots are representative of three independent experiments.

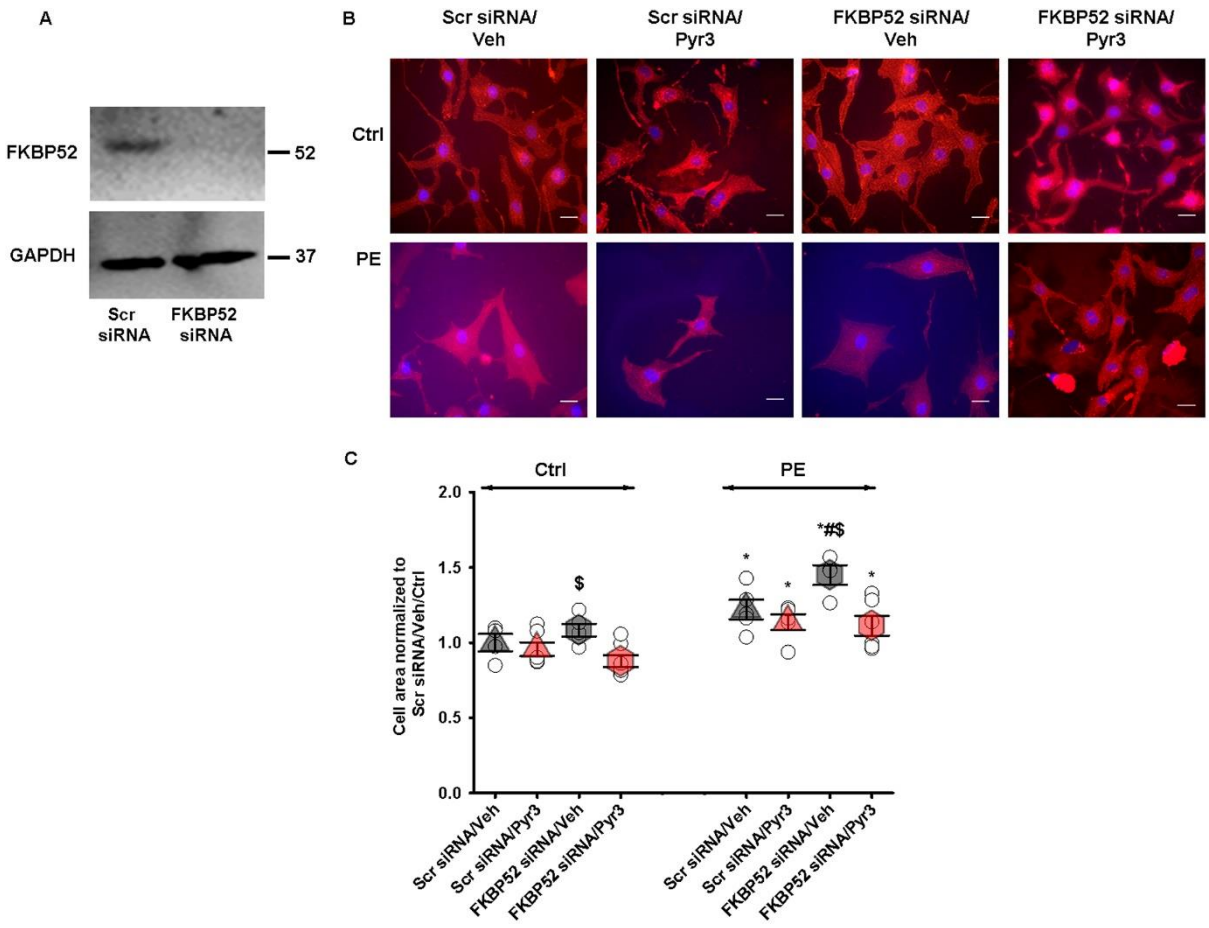

Fig. 3. Inhibition of TRPC3 attenuates cardiomyocyte hypertrophy induced by a down-regulation of FKBP52. (A) Neonatal rat cardiomyocytes (NRCs) were transfected with FKBP52 (FKBP52 siRNA) or scramble siRNAs (Scr siRNA). Confirmation of FKBP52 silencing in Western blotting. (B) The hypertrophic growth of NRCs was measured as an increase of the cell surface after phenylephrine (PE; 50 µM) or control (Ctrl) treatment for 24 h. Cells were treated with FKBP52 siRNA or scr siRNA ± pyrazole 3 (10 µM; Pyr3/vehicle (Veh)). Red: α-actinin; Blue: DAPI. Scale bar: 20 µm. Magnification, 63x. (C) Quantification of the cell area relative to Scr siRNA/Veh/Ctrl. *P<0.05 vs. respective Ctrl stimulation, $^{\#}$P<0.05 vs. Scr siRNA/Veh/PE, $^{\$}$P<0.05 vs. FKBP52 siRNA/Pyr3/Ctrl or PE, respectively (two-way Anova with Holm-Sidak method and unpaired t-test), *n* = 4-7, mean ± SEM.

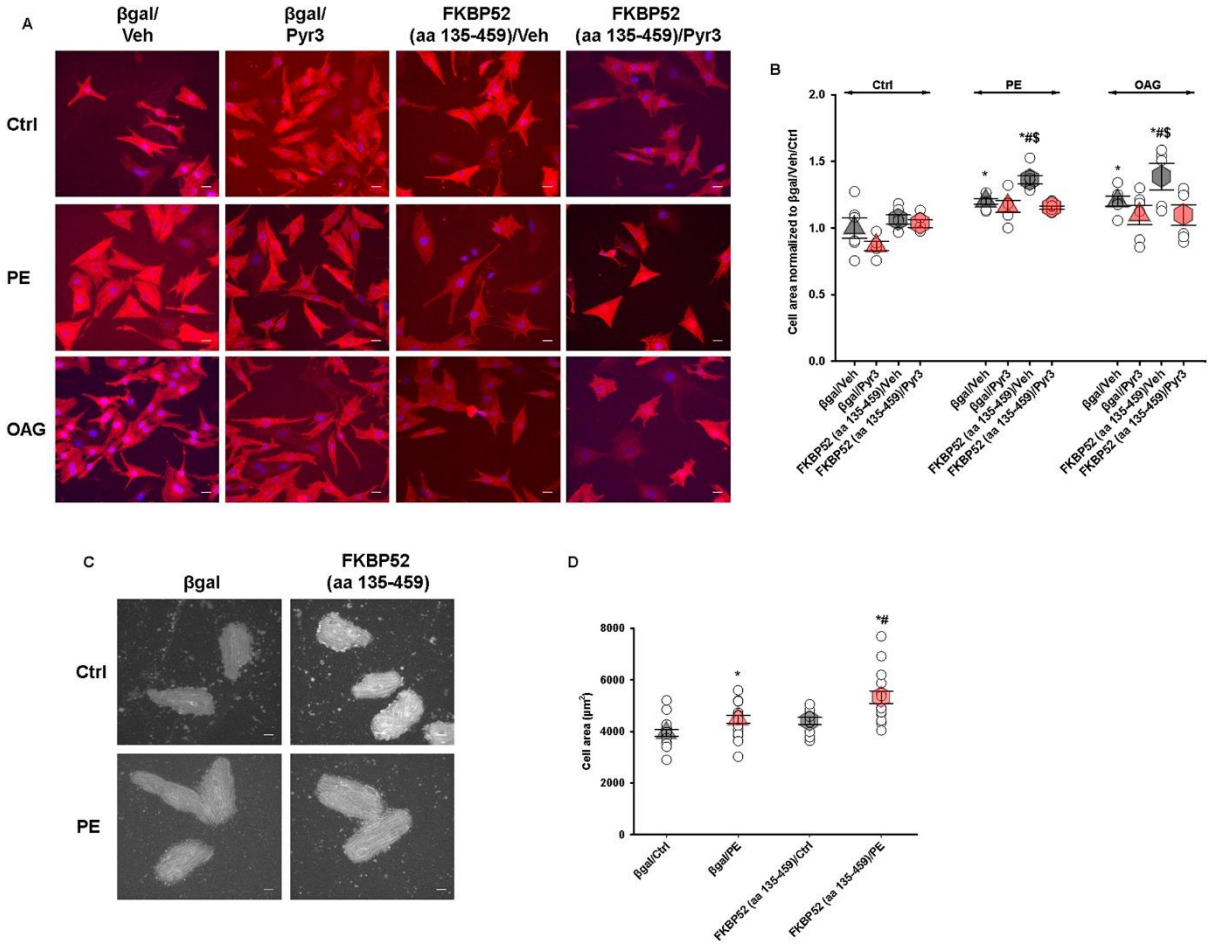

Fig 4. Overexpression of FKBP52 lacking the functional PPIase site promotes cardiomyocyte hypertrophy. (A) Neonatal rat cardiomyocytes (NRCs) were infected with adenoviruses encoding βgal or FKBP52 (aa 135-459) and treated with pyrazole 3 (10 µM; Pyr3) or vehicle (Veh). The cell area as indicator of the hypertrophic growth was analyzed after 24 h of phenylephrine (PE; 50 µM), 1-Oleoyl-2-acetyl-*sn*-glycerol (OAG, 100 µM) or control (Ctrl) stimulation. Red: α-actinin; Blue: DAPI. Scale bar: 20 µm. Magnification, 40x. (B) Quantification of the cell area relative to βgal-infected controls. *P<0.05 vs. respective Ctrl stimulation, $^{\#}$P<0.05 vs βgal/Veh/PE or βgal/Veh/OAG, $^{\$}$P<0.05 vs. FKBP52 (aa 135-459)/Pyr3 (two-way Anova with Holm-Sidak method and unpaired t-test), *n* = 5-7, mean ± SEM. (C) Adult rat cardiomyocytes infected with βgal or FKBP52 (aa 135-459) and stimulated with ± PE for 24 h. Scale bar: 20 µm. Magnification, 40x. (D) Quantification of the cell area relative to βgal-infected controls. *P<0.05 vs. respective Ctrl stimulation, $^{\#}$P<0.05 vs βgal/PE (two-way Anova with Holm-Sidak method), *n* = 11-17 cells, mean ± SEM.

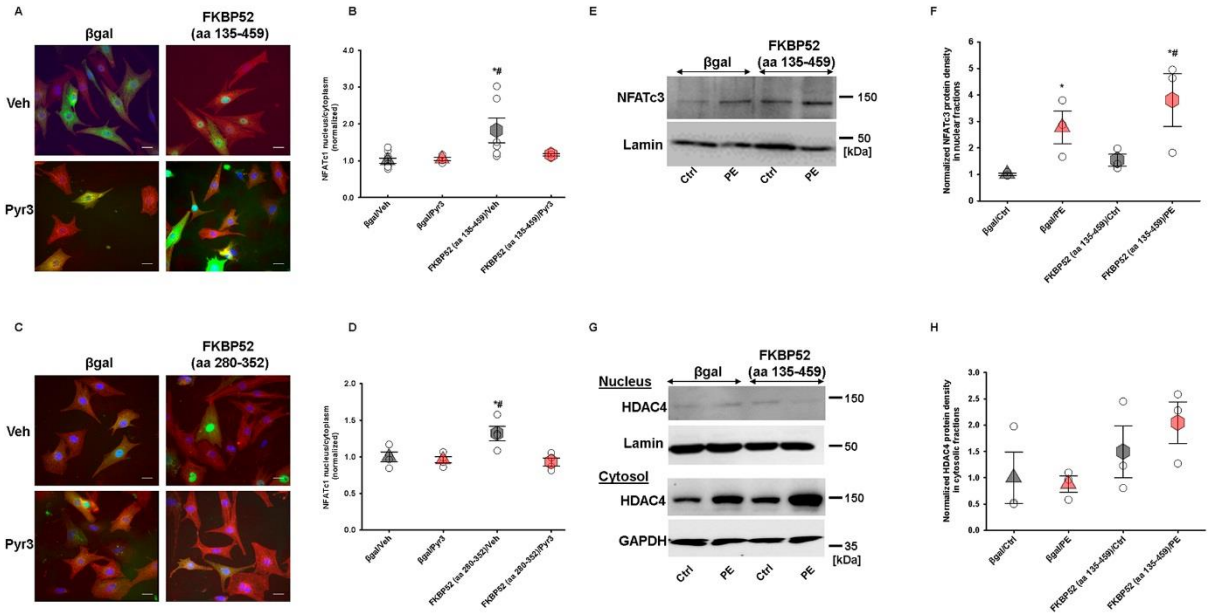

Fig 5. Overexpression of FKBP52 truncated mutants promotes NFAT signaling. (A) Neonatal rat cardiomyocytes (NRCs) were co-infected with adenoviruses encoding βgal or FKBP52 (aa 135-459), respectively, and NFATc1-GFP (green). Cells were pre-treated ± pyrazole 3 (10 µM; Pyr3/vehicle (Veh)). Localization of NFATc1 indicates the state of activity (in the nucleus (blue): transcriptionally active). Red: α-actinin. Scale bar: 20 µm. Magnification, 63x. (B) Quantification of NFATc1-GFP localized to the nucleus of NRCs. Average quantified values relative to βgal/Veh. *P<0.05 vs. βgal/Veh, #P<0.05 vs FKBP52 (aa 135-459)/Pyr3 (two-way Anova with Holm-Sidak method), *n* = 4-9, mean ± SEM. (C) NRCs co-infected with adenoviruses encoding βgal or FKBP52 (aa 280-352), respectively, and NFATc1-GFP (green). Red: α-actinin, Blue: DAPI. Pre-treatment with Pyr3 (10 µM) or Veh. Scale bar: 20 µm. Magnification, 63x. (D) Average quantified values relative to βgal/Veh. *P<0.05 vs. βgal/Veh, #P<0.05 vs FKBP52 (aa 280-352)/Pyr3 (two-way Anova with Holm-Sidak method), *n* = 4, mean ± SEM. (E) Western blot analysis of NFATc3 in nuclear extracts from NRCs overexpressing FKBP52 (aa 135-459) or βgal after 24 h of either phenylephrine (PE, 50 µM) or control (Ctrl) stimulation. (F) Quantification of protein expression levels. *P<0.05 vs. FKBP52 (aa 135-459)/Ctrl, #P<0.05 vs. βgal/PE (two-way Anova with Holm-Sidak method), *n* = 3, mean ± SEM. Lamin was used as loading control. (G) Western blot analysis of HDAC4 in nuclear and cytosolic extracts from (NRCs) overexpressing FKBP52 (aa 135-459) or βgal after 24 h of either PE or Ctrl stimulation. (H) Quantification of protein expression levels. n.s. (two-way Anova with Holm-Sidak method), *n* = 3, mean ± SEM. Lamin and GAPDH were used as loading controls.

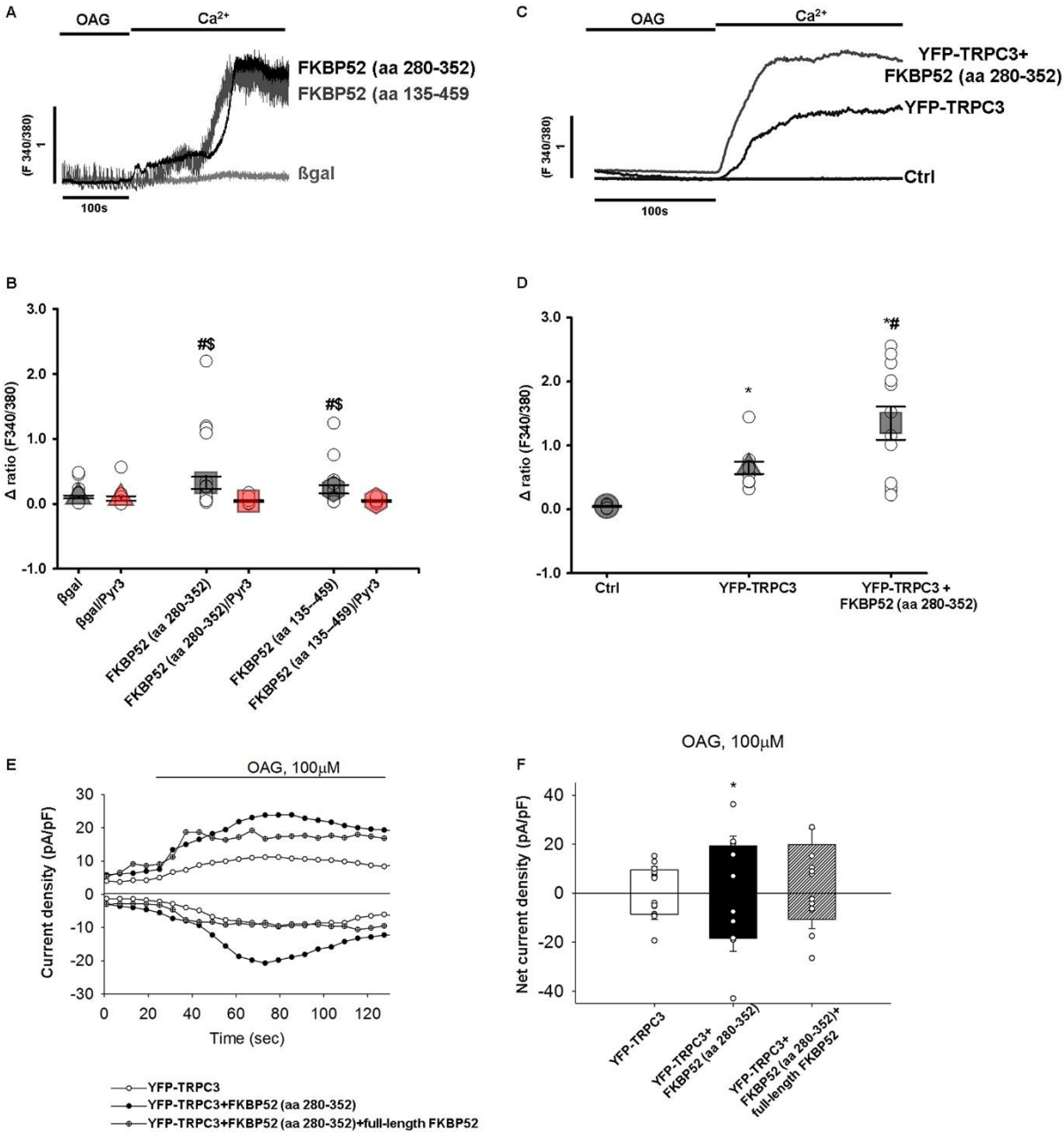

Fig. 6. Altered TRPC3-mediated Ca^{2+} signals and current densities upon expression of FKBP52 truncated mutants. (*A*) Representative Ca^{2+} recordings in NRCs overexpressing FKBP52 (aa 135-459), FKBP52 (aa 280-352) or βgal using Fura 2-AM. The cells were stimulated with 1-oleoyl-2-acetyl-*sn*-glycerol (OAG, 100 µM) in a nominally Ca^{2+}-free Tyrode solution which was followed by the re-addition of 2 mM Ca^{2+}. Note the increased Ca^{2+} response in the presence of FKBP52 (aa 135-459) and FKBP52 (aa 280-352). (B) Quantification of OAG-induced cytosolic Ca^{2+} signals in NRCs ± pyrazole 3 (Pyr3, 10 µM). Cells overexpressing FKBP52 (aa 135-459), FKBP52 (aa 280-352) or βgal were compared. Mean Δ ratio values were calculated by subtracting the peak value after Ca^{2+} re-addition from

the baseline value. $^{\#}$P<0.05 vs. βgal, $^{\$}$P<0.05 vs. FKBP52 (aa 135-459)/Pyr3 or FKBP52 (aa 280-352)/Pyr3, respectively (one-way Anova with Holm-Sidak method and unpaired t-test), *n* = 10-30, mean ± SEM. (C) Representative Ca^{2+} recordings in HEK 293 cells transfected with YFP-TRPC3, YFP-TRPC3 + FKBP52 (aa 280-352) or YFP (Ctrl). Stimulation with OAG (100 µM) in a nominally Ca^{2+}-free Tyrode solution and Ca^{2+} re-addition. (D) Quantification of OAG-induced cytosolic Ca^{2+} signals in HEK 293 cells expressing YFP (Ctrl), YFP-TRPC3 or TRPC3 + FKBP52 (aa 280-352), respectively. Mean Δ ratio values. *P<0.05 vs. Ctrl, $^{\#}$P<0.05 vs. YFP-TRPC3 (one-way Anova with Holm-Sidak method), *n* = 10-13, mean ± SEM. (E) Representative time course of the current development in HEK 293 cells transfected with YFP-TRPC3 (white), co-transfected with FKBP52 (aa 280-352; black) or co-transfected with FKBP52 (aa 280-352) and full-length FKBP52 (crossed) in response to OAG (100 µM). Current values were taken at -90 mV (inward) and at +70 mV (outward). (F) Mean values of the net current in HEK 293 cells expressing YFP-TRPC3 (white), YFP-TRPC3 + FKBP52 (aa 280-352; black or YFP-TRPC3 + FKBP52 (aa 280-352 + full-length FKBP52 (dashed), in response to OAG. Current values at -90 mV (inward) and at +70 mV (outward) were normalized by cell capacitance and indicated with circles for each condition. *P<0.05 vs. YFP-TRPC3 (one-way Anova with Holm-Sidak method), mean ± SEM.

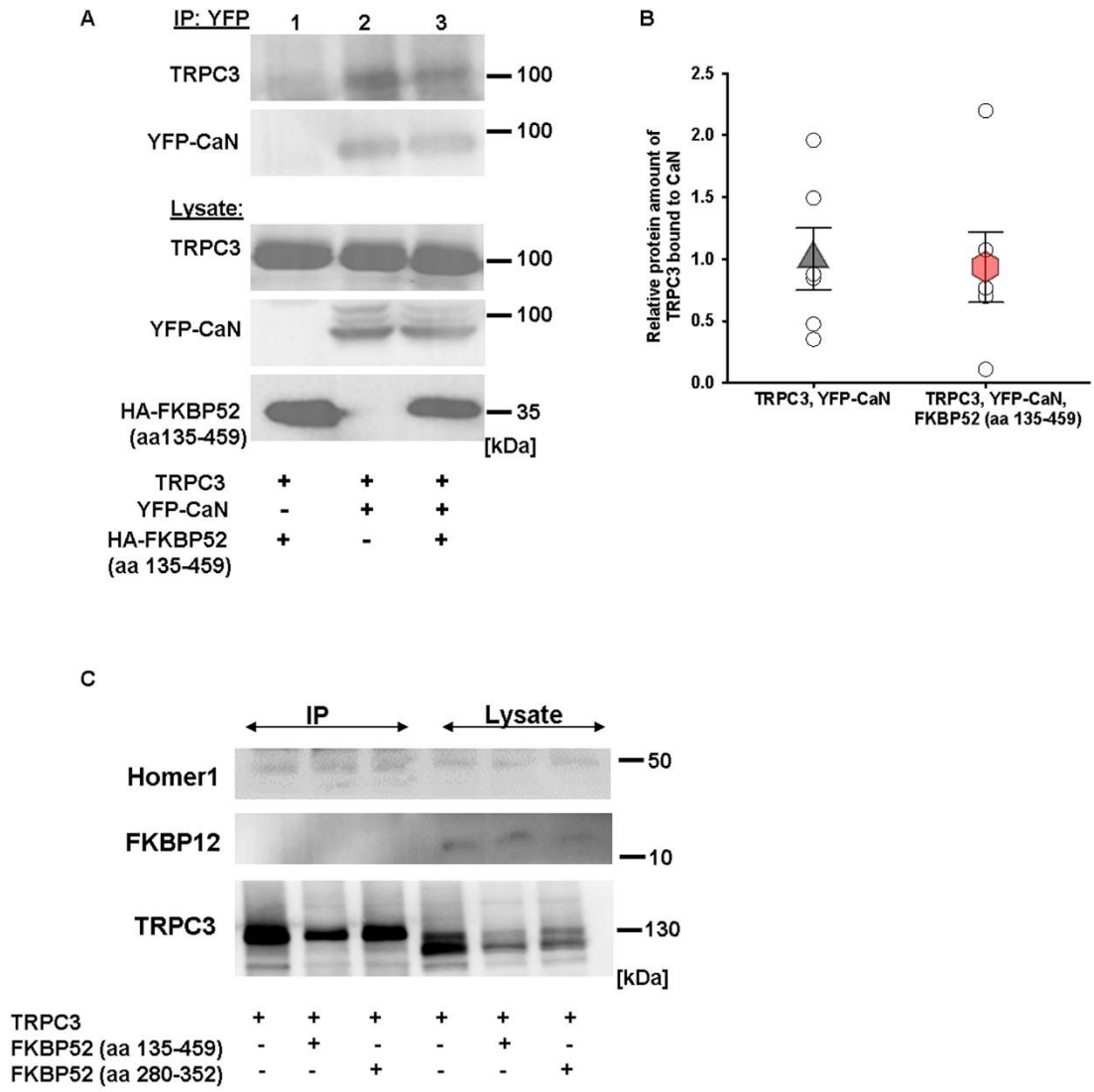

Fig. 7 Binding of TRPC3 with calcineurin, Homer1 or FKBP12 is not affected by FKBP52 truncated mutants. (A) Co-immunoprecipitation (Co-IP) of calcineurin (CaN) and TRPC3 in HEK 293 cells co-transfected with TRPC3, YFP-CaN together with HA-FKBP52 (aa 135-459) or an HA-control plasmid. TRPC3 was bound to CaN in cells expressing TRPC3 and YFP-CaN (2nd lane, 1st immunoblot) as well as in cells triple-transfected with TRPC3, YFP-CaN and HA-FKBP52 (aa 135-459; 3rd lane, 1st immunoblot). Representative immunoblots showing TRPC3 (1st blot) co-immunoprecipitated with YFP-CaN (2nd blot). Expression of TRPC3, YFP-CaN and HA-FKBP52 (aa 135-459) was confirmed in the respective lysates. (B) Densitometric quantification of the TRPC3 protein fraction bound to CaN. Values were calculated relative to the lysate. *P*=0.86; n.s. (one-way Anova with Holm-Sidak method), mean ± SEM. (C) Co-IP of YFP-TRPC3 and endogenously expressed Homer1 and FKBP12 in HEK 293 cells. Binding of Homer1 to YFP-TRPC3 is not affected by the expression of HA-FKBP52 (aa 135-459) or HA-

FKBP52 (aa 280-352). FKBP12 does not interact with YFP-TRPC3. The blots are representative of three independent experiments.

Table 1 Clones from a cardiac mouse cDNA library recovered with either the N-terminus (aa 1-341) or the C-terminal fragment (aa 742-848) of TRPC3 in a Ras recruitment yeast two-hybrid screen.

Protein interactions with the N-terminus (aa 1-341) of TRPC3:
Myosin light chain regulatory B like
Myosin light chain polypeptide 2
Desmin
Myomesin
Creatine kinase, mitochondrial sarcomeric
Mitochondrial Aconitase
Translocase of inner mitochondrial membrane 44
Triosephosphate isomerase
Protein interactions with the C-terminus (aa 742-848) of TRPC3:
FKBP12
Myosin light chain polypeptide 2
Pre-B-cell leukemia transcription factor interacting protein 1
Triosephosphate isomerase

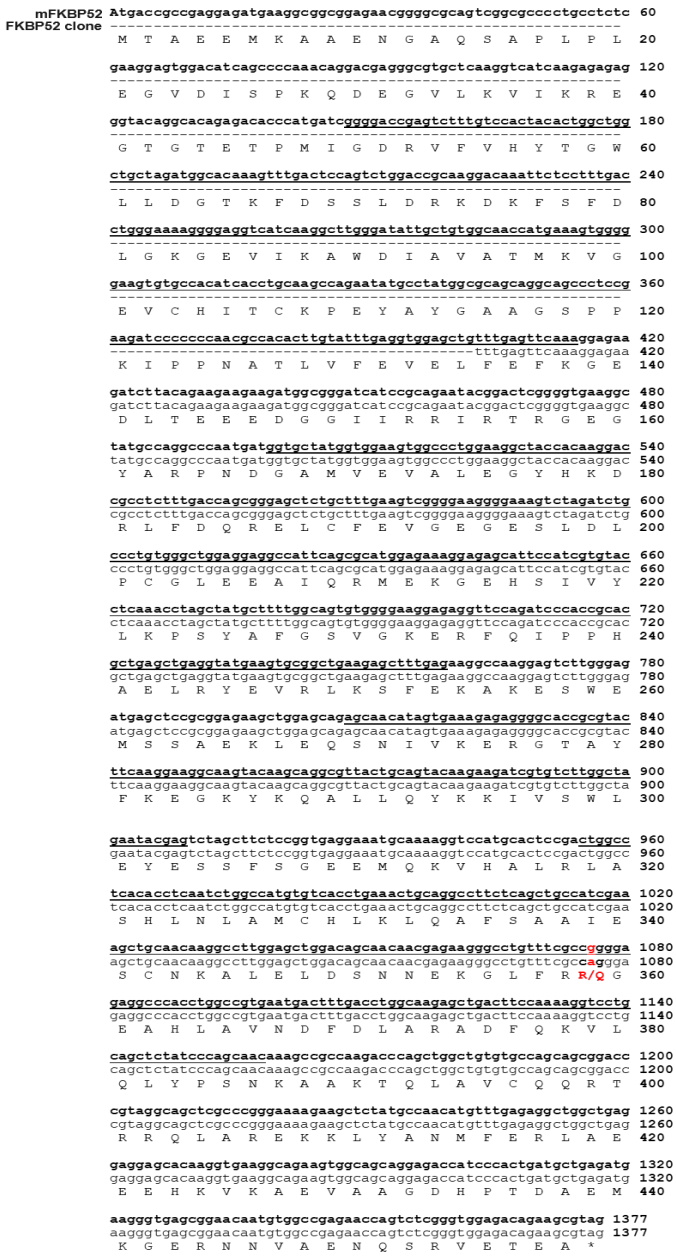

Fig. S1. **Sequence alignment of mouse FKBP52 (mFKBP52) and the FKBP52 cDNA clone from the screen.** Underlined sequences represent FKBP52 domains. The point mutation G1075A in the FKBP52 clone is marked in red.

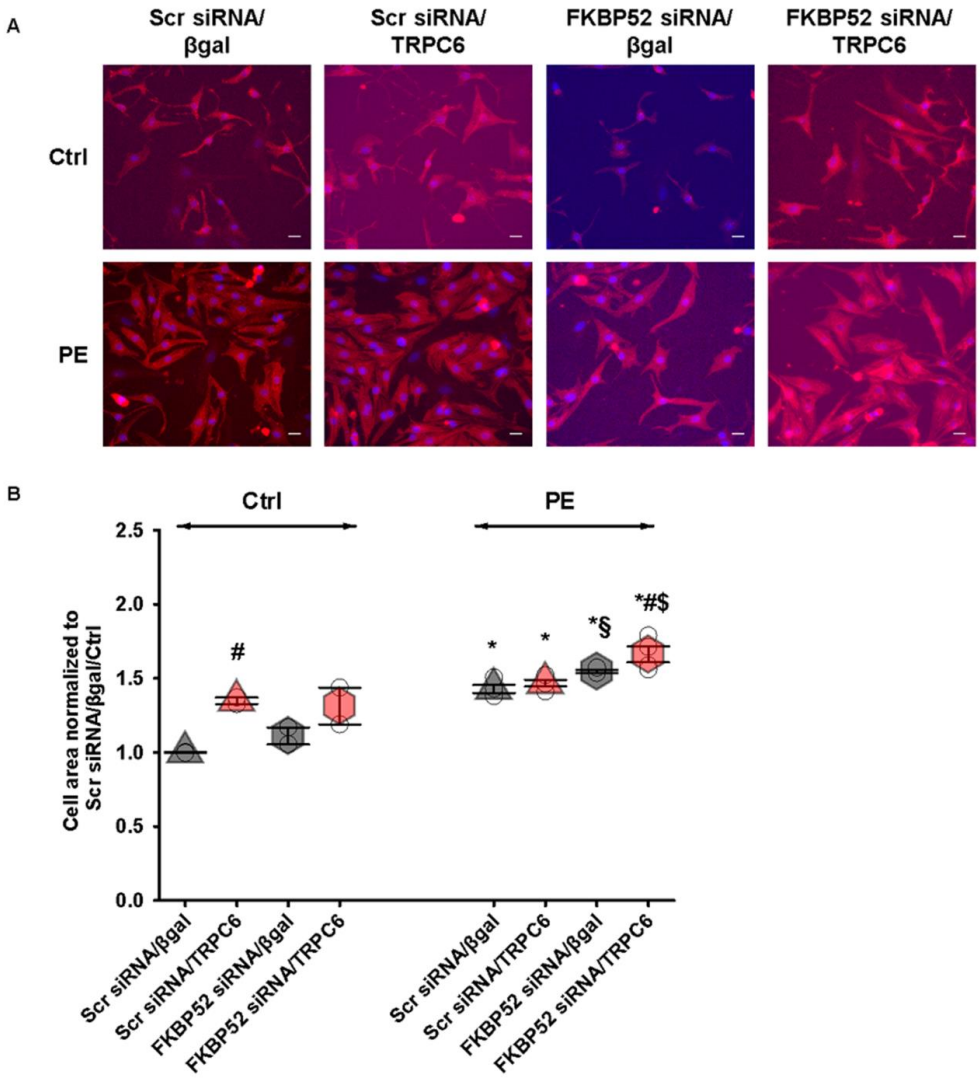

Fig. S2. Downregulation of FKBP52 results in an elevated TRPC6-induced hypertrophic response. (A) Neonatal rat cardiomyocytes (NRCs) were infected with adenoviruses encoding βgal or TRPC6 and transfected with FKBP52 (FKBP52 siRNA) or scramble siRNAs (Scr siRNA). The hypertrophic growth of NRCs was measured as an increase of the cell surface after phenylephrine (PE; 50 µM) or control (Ctrl) stimulation for 24 h. Red: α-actinin; Blue: DAPI. Scale bar: 20 µm. Magnification, 40x. (B) Quantification of the cell area relative to Scr siRNA/βgal/Ctrl. *P<0.05 vs. respective Ctrl stimulation, $^{\#}$P<0.05 vs. Scr siRNA/βgal/Ctrl or vs. FKBP52 siRNA/βgal/PE, respectively, §P<0.05 vs. Scr siRNA/ βgal/PE, $^{\$}$P<0.05 vs. FKBP52 siRNA/ βgal/PE (two-way Anova with Holm-Sidak method and unpaired t-test), *n* = 2-4, mean ± SEM.

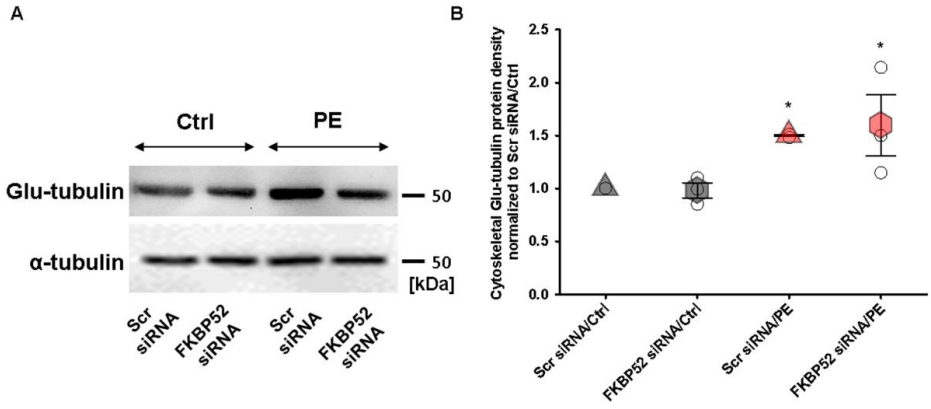

Fig S3. The stabilization of microtubules is not affected by a downregulation of FKBP52 during hypertrophic stimulation. (A) Western blot analysis of α-tubulin and Glu-tubulin expression levels in cytoskeletal extracts from neonatal rat cardiomyocytes (NRCs) after 24 h of phenylephrine (PE) or control (Ctrl) stimulation. The cells were transfected with FKBP52 or scramble siRNAs (Scr siRNA). (B) PE stimulation results in increased Glu-tubulin expression levels in FKBP52 and scr siRNA-treated NRCs. Protein expression levels were normalized to scr siRNA/Ctrl. *P<0.05 vs. to scr siRNA/Ctrl or FKBP52 siRNA /Ctrl, respectively (two-way Anova with Holm-Sidak method), *n* = 3, mean ± SEM.

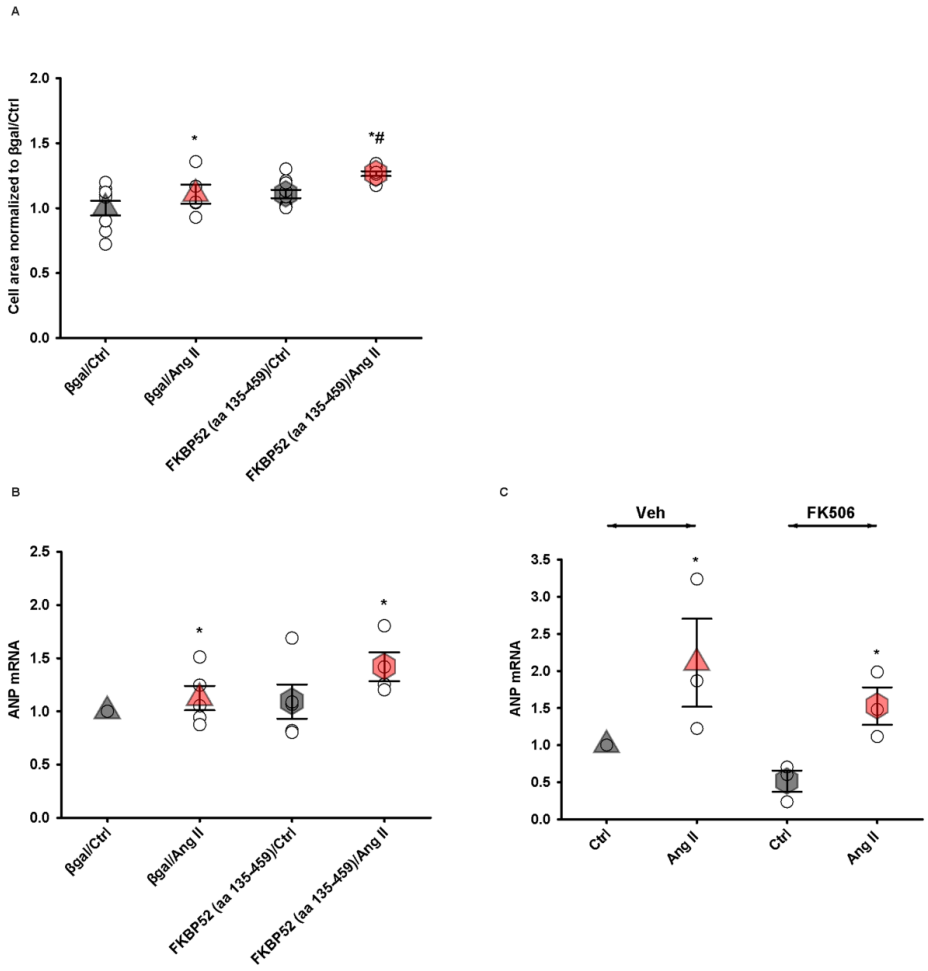

Fig S4. FKBP52 (aa 135-459) affects an angiotensin II-stimulated hypertrophic response differently than FK506. (A) Quantification of the cell area after 24 h of angiotensin II (Ang II; 100 nM) or control (Ctrl) stimulation. NRCs were infected with FKBP52 (aa 135-459) or βgal. Data are shown relative to βgal-infected controls. *P<0.05 vs. βgal/Ctrl, #P<0.05 vs. βgal/Ang II (two-way Anova with Holm-Sidak method), *n* = 5-9, mean ± SEM. (B) mRNA levels of atrial natriuretic peptide (ANP) were determined after 24 h of Ang II or control (Ctrl) stimulation *via* qPCR from NRCs expressing βgal or FKBP52 (aa 135-459). *P<0.05 vs. βgal or FKBP52 (aa 135-459)/Ctrl (two-way Anova with Holm-Sidak method), *n* = 4-5, mean ± SEM. (C) mRNA levels from NRCs treated with FK506 (2 µM) or vehicle (Veh). *P<0.05 vs. Ctrl (two-way Anova with Holm-Sidak method), *n* = 3, mean ± SEM. *P<0.05.

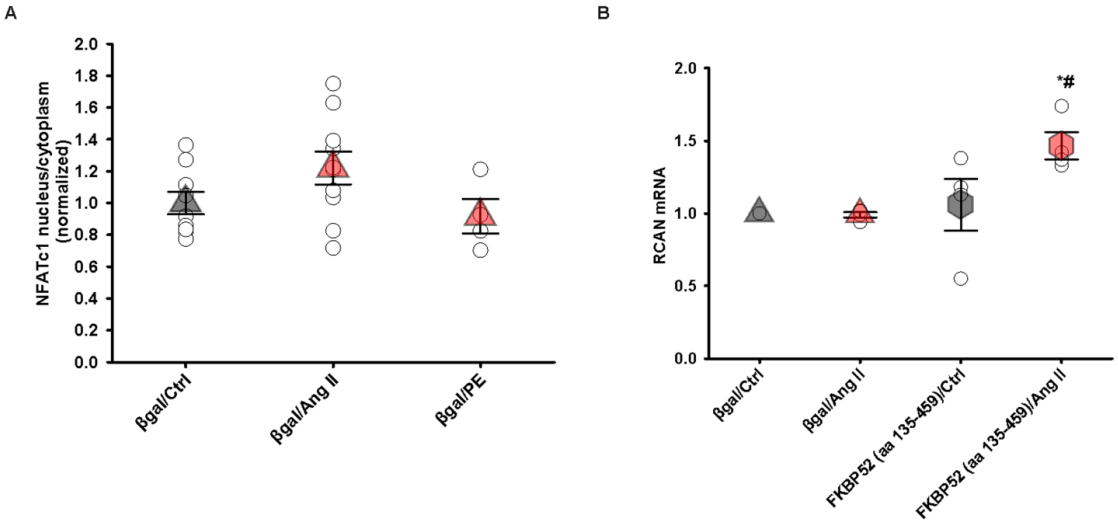

Fig. S5. NFATc1 and RCAN activation in response to agonist stimulation in neonatal rat cardiomyocytes. (A) Average quantified values of NFATc1-GFP localized to the nucleus in response to Ang II (Ang II; 100 nM), phenylephrine (PE; 50 µM) or control (Ctrl) stimulation. Neonatal rat cardiomyocytes (NRCs) were infected with βgal. Data are shown relative to βgal/Ctrl (One-way Anova with Holm-Sidak method), *n* = 4-10, mean ± SEM. (B) Regulator of calcineurin 1 (RCAN) expression levels as parameter of the activation of calcineurin in NRCs. mRNA levels of RCAN were measured after 24 h of Ang II or control (Ctrl) stimulation *via* qPCR. NRCs were infected with βgal or FKBP52 (aa 135-459). Average quantified values relative to βgal/Ctrl. *P<0.05 vs. FKBP52 (aa 135-459)/Ctrl, $^{\#}$P<0.05 vs. βgal/ Ang II (two-way Anova with Holm-Sidak method), *n* = 4, mean ± SEM.

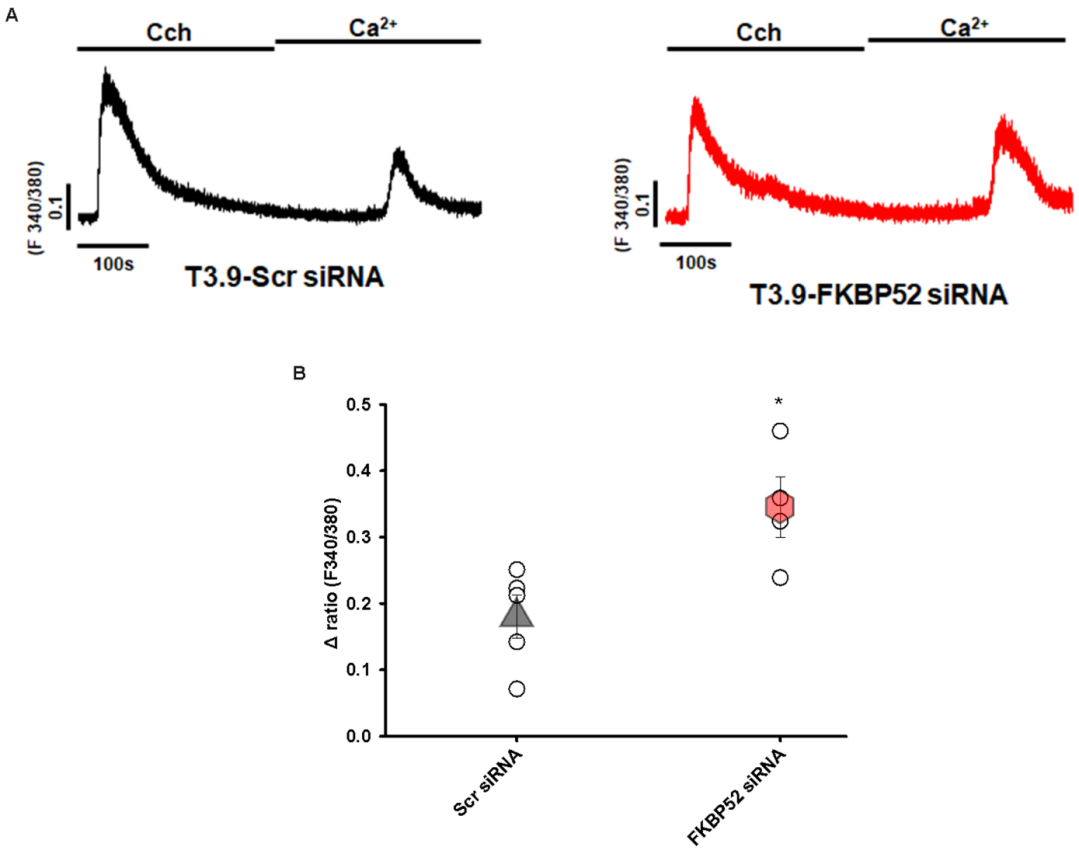

Fig. S6. TRPC3-dependent Ca^{2+} signals in HEK 293 cells are dependent on FKBP52. (A) Representative Ca^{2+} recordings of HEK 293 cells stably expressing TRPC3 (T3.9). The cells were treated with scramble (Scr siRNA) or FKBP52 siRNAs. A TRPC3-related Ca^{2+} influx was measured according to a classical Ca^{2+} re-addition protocol. T3.9 cells were first stimulated with the G_q protein-coupled receptor agonist carbachol (Cch, 300 µM) in nominally Ca^{2+}-free conditions and subsequently perfused with an external solution containing $CaCl_2$. This manoeuvre resulted in a Cch-dependent Ca^{2+} release from internal stores followed by a Ca^{2+} influx from the extracellular space. The TRPC3-mediated Ca^{2+} influx was significantly enhanced in cells treated with siRNAs against FKBP52. (B) Mean Δ ratio values were calculated by subtracting the peak value after Ca^{2+} re-addition from the baseline value *P<0.05 vs. Scr siRNA (unpaired t-test), *n* = 4-5, mean ± SEM. The mean Δ ratio of the Ca^{2+} release (peak-baseline) was not different between the groups. P= 0.34.

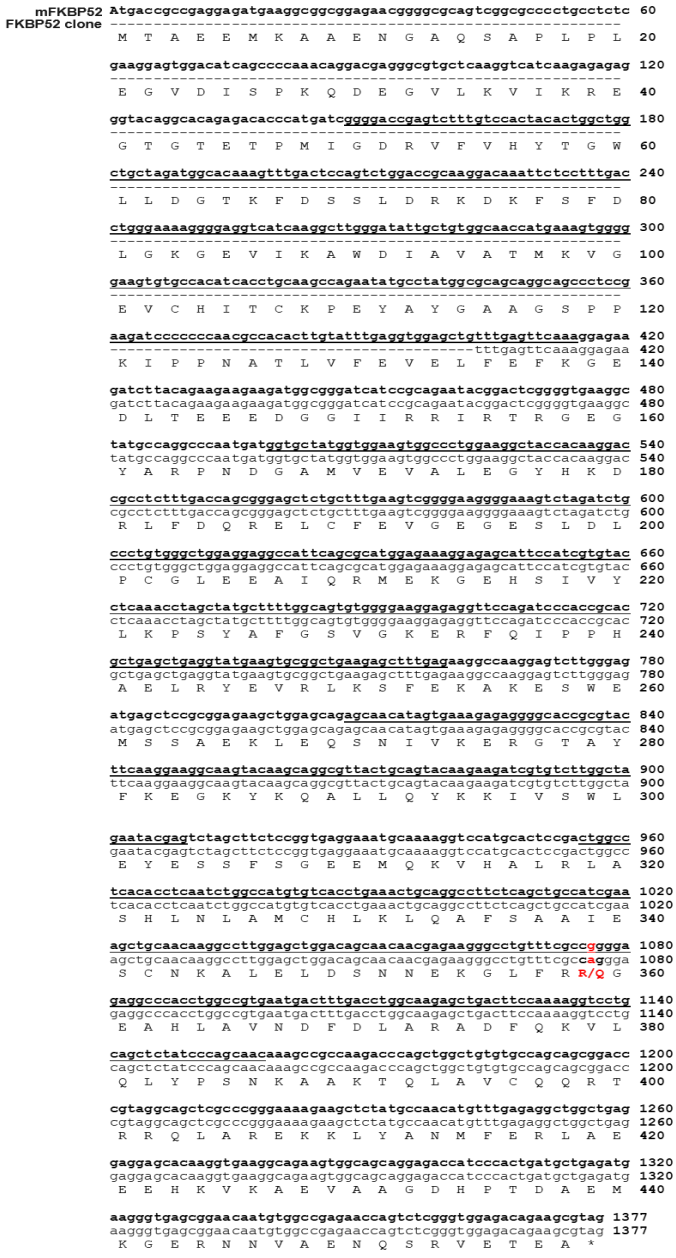

Fig. S1. **Sequence alignment of mouse FKBP52 (mFKBP52) and the FKBP52 cDNA clone from the screen.** Underlined sequences represent FKBP52 domains. The point mutation G1075A in the FKBP52 clone is marked in red.

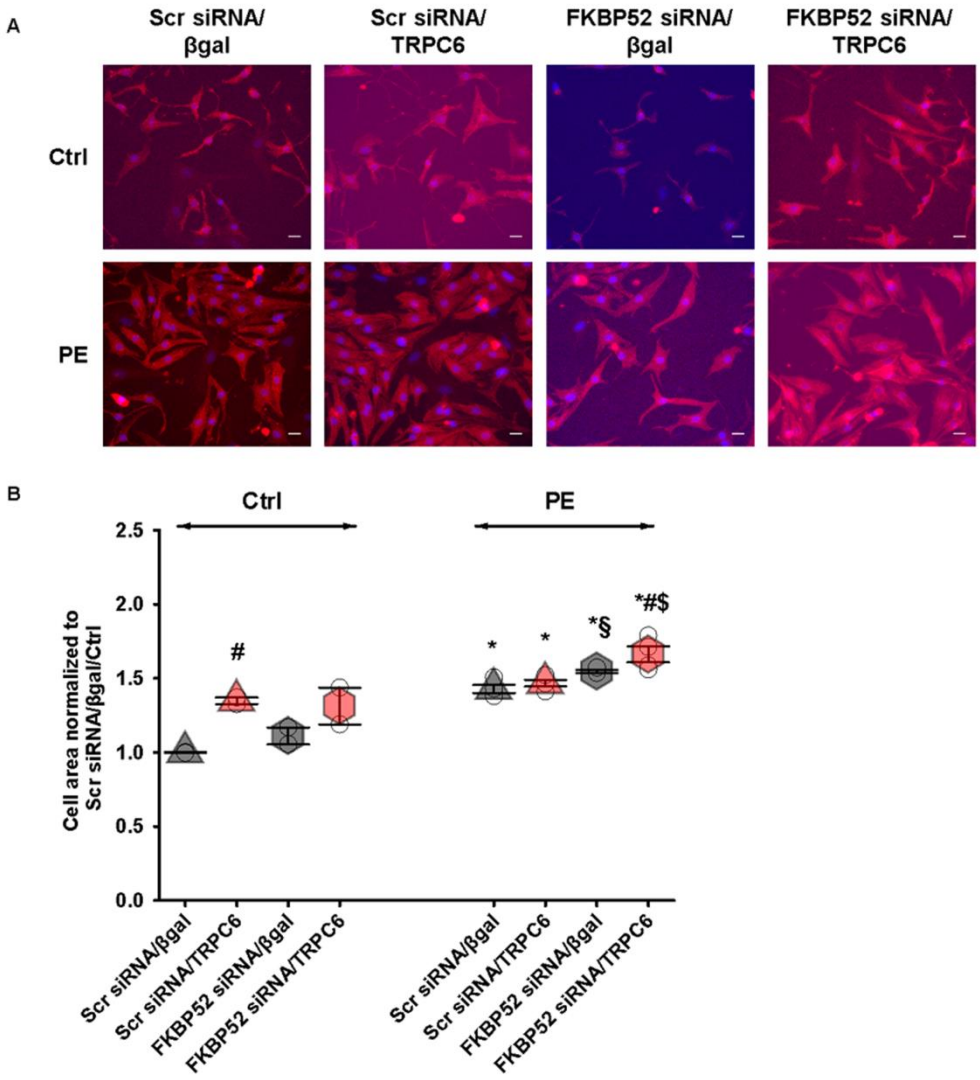

Fig. S2. Downregulation of FKBP52 results in an elevated TRPC6-induced hypertrophic response. (A) Neonatal rat cardiomyocytes (NRCs) were infected with adenoviruses encoding βgal or TRPC6 and transfected with FKBP52 (FKBP52 siRNA) or scramble siRNAs (Scr siRNA). The hypertrophic growth of NRCs was measured as an increase of the cell surface after phenylephrine (PE; 50 µM) or control (Ctrl) stimulation for 24 h. Red, α-actinin; Blue, DAPI. Scale bar: 20 µm. Taken with a 40× magnification objective. (B) Quantification of the cell area relative to Scr siRNA/βgal/Ctrl. *P<0.05 vs. respective Ctrl stimulation, $^{\#}$P<0.05 vs. Scr siRNA/βgal/Ctrl or vs. FKBP52 siRNA/βgal/PE, respectively, §P<0.05 vs. Scr siRNA/ βgal/PE, $^{\$}$P<0.05 vs. FKBP52 siRNA/ βgal/PE (two-way Anova with Holm-Sidak method and unpaired t-test), *n* = 2-4, mean ± SEM.

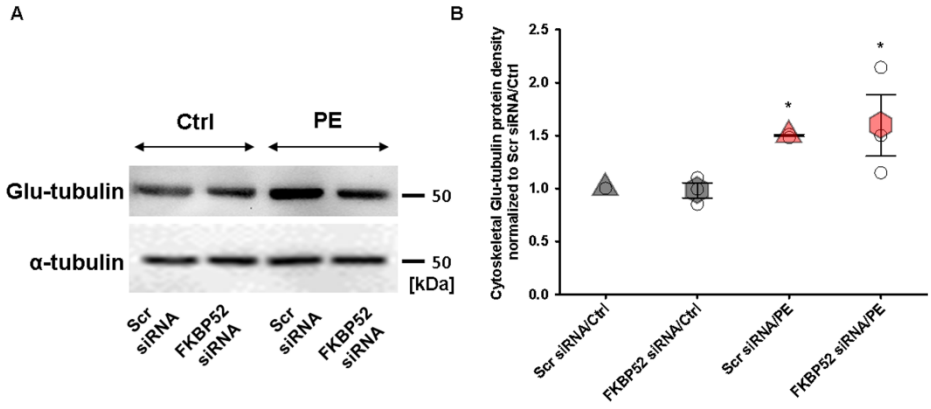

Fig S3. The stabilization of microtubules is not affected by a downregulation of FKBP52 during hypertrophic stimulation. (A) Western blot analysis of α-tubulin and Glu-tubulin expression levels in cytoskeletal extracts from neonatal rat cardiomyocytes (NRCs) after 24 h of phenylephrine (PE) or control (Ctrl) stimulation. The cells were transfected with FKBP52 or scramble siRNAs (Scr siRNA). (B) PE stimulation results in increased Glu-tubulin expression levels in FKBP52 and scr siRNA-treated NRCs. Protein expression levels were normalized to scr siRNA/Ctrl. *P<0.05 vs. to scr siRNA/Ctrl or FKBP52 siRNA /Ctrl, respectively (two-way Anova with Holm-Sidak method), *n* = 3, mean ± SEM.

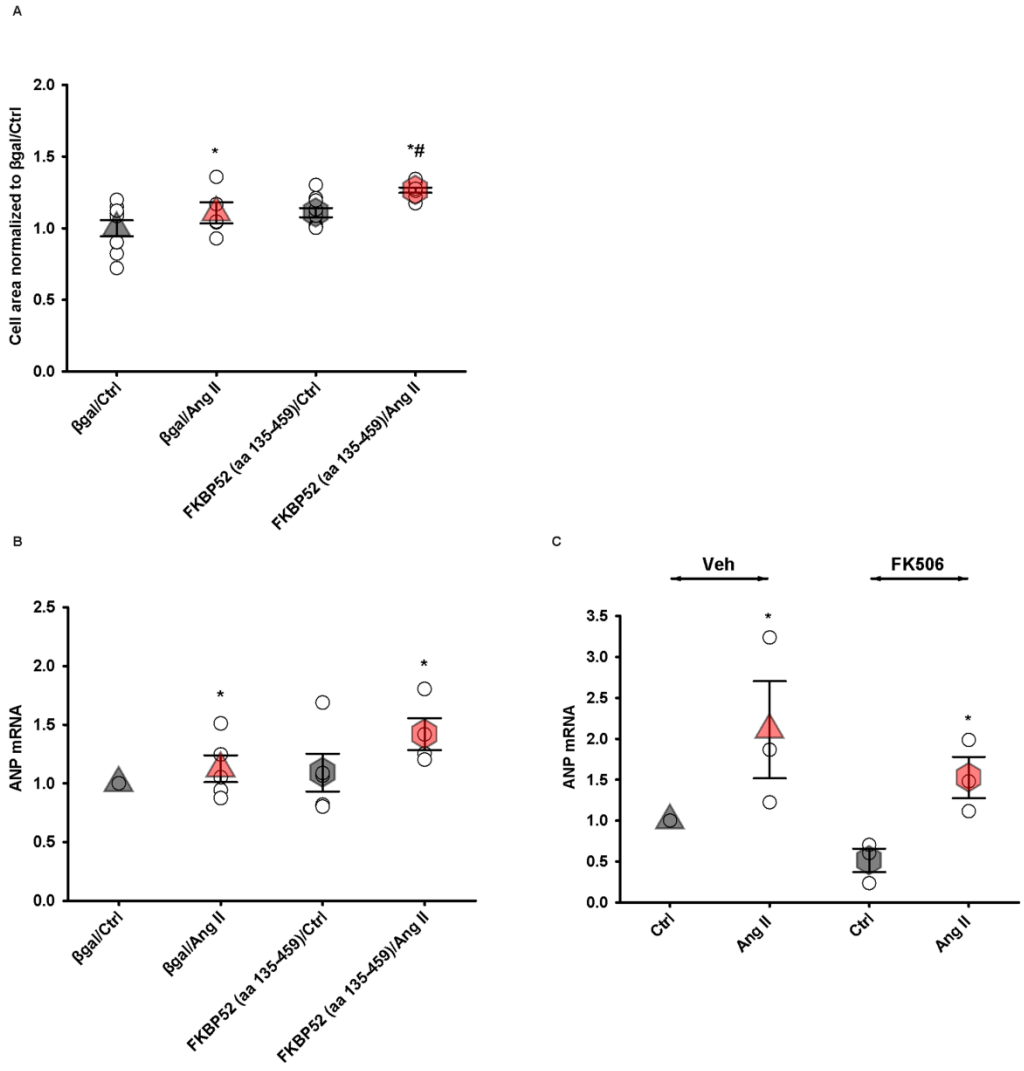

Fig S4. FKBP52 (aa 135-459) affects an angiotensin II-stimulated hypertrophic response differently than FK506. (A) Quantification of the cell area after 24 h of angiotensin II (Ang II; 100 nM) or control (Ctrl) stimulation. NRCs were infected with FKBP52 (aa 135-459) or βgal. Data are shown relative to βgal-infected controls. *P<0.05 vs. βgal/Ctrl, #P<0.05 vs. βgal/Ang II (two-way Anova with Holm-Sidak method), *n* = 5-9, mean ± SEM. (B) mRNA levels of atrial natriuretic peptide (ANP) were determined after 24 h of Ang II or control (Ctrl) stimulation *via* qPCR from NRCs expressing βgal or FKBP52 (aa 135-459). *P<0.05 vs. βgal or FKBP52 (aa 135-459)/Ctrl (two-way Anova with Holm-Sidak method), *n* = 4-5, mean ± SEM. (C) mRNA levels from NRCs treated with FK506 (2 µM) or vehicle (Veh). *P<0.05 vs. Ctrl (two-way Anova with Holm-Sidak method), *n* = 3, mean ± SEM. *P<0.05.

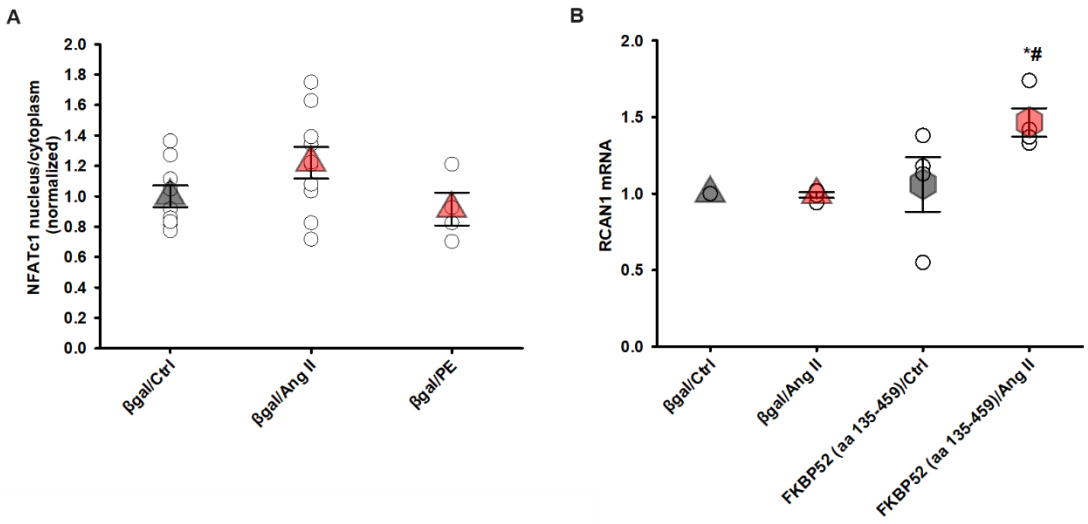

Fig. S5. NFATc1 and RCAN1 activation in response to agonist stimulation in neonatal rat cardiomyocytes. (A) Average quantified values of NFATc1-GFP localized to the nucleus in response to angiotensin II (Ang II; 100 nM), phenylephrine (PE; 50 µM) or control (Ctrl) stimulation. Neonatal rat cardiomyocytes (NRCs) were infected with βgal. Data are shown relative to βgal/Ctrl (One-way Anova with Holm-Sidak method), *n* = 4-10, mean ± SEM. (B) Regulator of calcineurin 1 (RCAN1) expression levels as parameter of the activation of calcineurin in NRCs. mRNA levels of RCAN1 were measured after 24 h of Ang II or control (Ctrl) stimulation *via* qPCR. NRCs were infected with βgal or FKBP52 (aa 135-459). Average quantified values relative to βgal/Ctrl. *P<0.05 vs. FKBP52 (aa 135-459)/Ctrl, $^{\#}$P<0.05 vs. βgal/ Ang II (two-way Anova with Holm-Sidak method), *n* = 4, mean ± SEM.

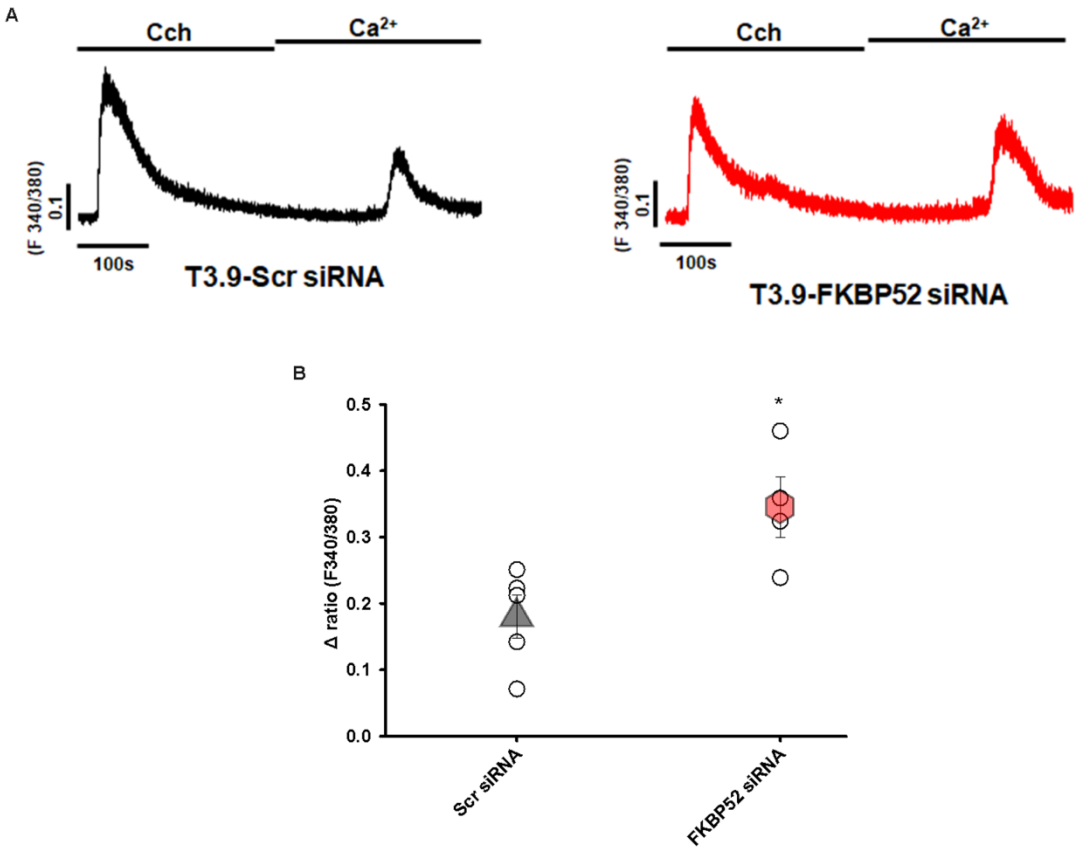

Fig. S6. TRPC3-dependent Ca^{2+} signals in HEK 293 cells are dependent on FKBP52. (A) Representative Ca^{2+} recordings of HEK 293 cells stably expressing TRPC3 (T3.9). The cells were treated with scramble (Scr siRNA) or FKBP52 siRNAs. A TRPC3-related Ca^{2+} influx was measured according to a classical Ca^{2+} re-addition protocol. T3.9 cells were first stimulated with the G_q protein-coupled receptor agonist carbachol (Cch, 300 µM) in nominally Ca^{2+}-free conditions and subsequently perfused with an external solution containing $CaCl_2$. This manoeuvre resulted in a Cch-dependent Ca^{2+} release from internal stores followed by a Ca^{2+} influx from the extracellular space. The TRPC3-mediated Ca^{2+} influx was significantly enhanced in cells treated with siRNAs against FKBP52. (B) Mean Δ ratio values were calculated by subtracting the peak value after Ca^{2+} re-addition from the baseline value *P<0.05 vs. Scr siRNA (unpaired t-test), *n* = 4-5, mean ± SEM. The mean Δ ratio of the Ca^{2+} release (peak-baseline) was not different between the groups. P= 0.34.